Canadian Journal of Earth Sciences
Revue canadienne des sciences de la Terre

THE TWO-STAGE AEGEAN EXTENSION, FROM LOCALIZED TO DISTRIBUTED, A RESULT OF SLAB ROLLBACK ACCELERATION

Journal:	*Canadian Journal of Earth Sciences*
Manuscript ID	cjes-2015-0203.R1
Manuscript Type:	Article
Date Submitted by the Author:	17-Jan-2016
Complete List of Authors:	Brun, Jean-Pierre; University Rennes 1, Géosciences Rennes Faccenna, Claudio; Università Roma Tre, Laboratory of Experimental Tectonics Gueydan, Frédéric; Université de Montpellier, Géosciences Montpellier Sokoutis, Dimitrios; Utrecht University, Department of Earth Sciences; University of Oslo, Department of Geosciences Philippon, Mélody; Université des Antilles, Géosciences Montpellier Kydonakis , Konstantinos ; Université Rennes 1, Géosciences Rennes Gorini, Christian; UPMC Université Paris 06, ISTeP
Keyword:	Hellenic subduction, slab rollback, trench retreat, Aegean back-arc extension

THE TWO-STAGE AEGEAN EXTENSION, FROM LOCALIZED TO DISTRIBUTED, A RESULT OF SLAB ROLLBACK ACCELERATION

Jean-Pierre Brun, Claudio Faccenna, Frédéric Gueydan, Dimitrios Sokoutis, Mélody Philippon, Konstantinos Kydonakis and Christian Gorini.

J.-P. Brun. Université Rennes 1, Géosciences Rennes,UMR 6118 CNRS, bat. 15 - Campus de Beaulieu, 263 Av du général Leclerc, BP 74205, 35042, Rennes Cedex, France. Jean-Pierre.Brun@univ-rennes1.fr

C. Faccenna. LET, Laboratory of Experimental Tectonics, Università Roma Tre, Rome, Italy. claudio.faccenna@uniroma3.it

F. Gueydan. Université de Montpellier. Géosciences Montpellier, UMR5243, Université de Montpellier, Rue Eugène Bataillon, France. frederic.gueydan@univ-montp2.fr

D. Sokoutis. Department of Earth Sciences, Faculty of Geosciences, Utrecht University, Budapestlaan 4, PO Box 80021, 3508 Utrecht, The Netherlands and Department of Geosciences, University of Oslo, PO Box 1047, Blindern, N-0316 Oslo, Norway. D.Sokoutis@uu.nl

M. Philippon. Université des Antilles, Géosciences Montpellier, UMR 5243, Campus de Fouillole, 97159, Pointe à Pitre, France. Melodie.Philippon@gm.univ-montp2.fr

K. Kydonakis. Université Rennes 1, Géosciences Rennes,UMR 6118 CNRS, bat. 15 - Campus de Beaulieu, 263 Av du général Leclerc, BP 74205, 35042, Rennes Cedex, France. konstantinos.kydonakis@univ-rennes1.fr

C. Gorini. Sorbonne Universités, UPMC Univ Paris 06, UMR 7193, ISTeP, F-75005, Paris, France. christian.gorini@upmc.fr

Abstract: Back-arc extension in the Aegean, which was driven by slab rollback since 45 Ma, is described here for the first time in two stages. From Middle Eocene to Middle Miocene, deformation was localized leading to i) the exhumation of high-pressure metamorphic rocks to crustal depths, ii) the exhumation of high-temperature metamorphic rocks in core complexes and iii) the deposition of sedimentary basins. Since Middle Miocene, extension distributed over the whole Aegean domain controlled the deposition of onshore and offshore Neogene sedimentary basins. We reconstructed this two-stage evolution in 3D and four steps at Aegean scale by using available ages of metamorphic and sedimentary processes, geometry and kinematics of ductile deformation, paleomagnetic data and available tomographic models. The restoration model shows that the rate of trench retreat was around 0.6 cm/y during the first 30 My and then accelerated up to 3.2 cm/y during the last 15 My. The sharp transition observed in the mode of extension, localized versus distributed, in Middle Miocene correlates with the acceleration of trench retreat and is likely a consequence of the Hellenic slab tearing documented by mantle tomography. The development of large dextral NE-SW strike-slip faults, since Middle Miocene, is illustrated by the 450 Km-long fault zone, offshore from Myrthes to Ikaria and onshore from Izmir to Balikeshir, in western Anatolia. Therefore, the interaction between the Hellenic trench retreat and the westward displacement of Anatolia started in Middle Miocene, almost 10 Ma before the propagation of the North Anatolian Fault in the North Aegean.

Keywords: Hellenic subduction, slab rollback, trench retreat, Aegean back-arc extension

Résumé: L'extension égéenne, mue par le recul de la subduction Hellénique, est un processus qui, depuis 45 Ma, montre une évolution en deux stades. De l'Eocène moyen au Miocène moyen, la déformation localisée est matérialisée par i) l'exhumation de roches métamorphiques de haute pression, ii) l'exhumation de roches de haute température dans des "core complexes" et iii) le dépôt de bassins sédimentaires Paléogènes. Depuis le Miocène moyen, l'extension est distribuée dans tout le domaine égéen contrôle le développement de bassins sédimentaires Néogènes. Cette évolution en deux stades à l'échelle de l'ensemble du domaine égéen est reconstruite en utilisant les âges des processus métamorphiques et sédimentaires, la cinématique de la déformation ductile, les données paléomagnétiques existantes et les modèles tomographiques les plus récents. Le modèle de restauration montre que la vitesse de recul de la subduction, de 0,6 cm/an pendant les premiers 30 Ma, s'est accélérée au Miocène moyen pour atteindre 3.2 cm/an au cours des derniers 15 Ma. La transition localisée-distribuée de l'extension au Miocène moyen, corrélée avec l'accélération du recul de la fosse, est probablement une conséquence de la déchirure du panneau de lithosphère subductée. Le développement de grands décrochements dextres orientés NE-SW pendant le deuxième stade d'extension indique que l'interaction entre le recul de la subduction Hellénique et le déplacement vers l'Ouest de l'Anatolie a débuté au Miocène moyen, 10 Ma avant l'arrivée de la Faille Nord Anatolienne dans le Nord de l'Egée.

Introduction

The Aegean Tertiary tectonic history corresponds to back-arc extension driven by slab rollback (Royden 1993; Jolivet and Faccenna 2000; Faccenna et al. 2003, 2014, Brun and Faccenna 2008). Extension started around 45 Ma ago (Brun and Sokoutis 2010) and accommodated up to 600 km of trench retreat (Jolivet and Brun, 2010; Jolivet et al. 2013). Extension followed the closure of Vardar and Pindos oceanic domains in Cretaceous-Eocene (Dercourt et al. 1993; Channell and Kozur 1997; Robertson 2004) that led to the stacking of three continental blocks: Rhodopia, Pelagonia and Adria, from top to base (Fig. 1). Tomographic models of the underlying mantle image a single slab (Wortel and Spakman 2000; Piromallo and Morelli 2003; Widiyantoro et al. 2004) indicating that the convergence of continental blocks, now separated by two suture zones, has been accommodated by a single subduction (Faccenna et al. 2003).

The first plate kinematic models of eastern Mediterranean (McKenzie 1972, 1978; Le Pichon and Angelier 1981) and the present-day displacement field from satellite geodesy (McClusky et al. 2000; Hollenstein et al. 2008; Müller et al. 2013) show that the active pattern of extension combines the effects of the southwestward retreat of the Hellenic trench and the westward displacement of Anatolia along the North Anatolian Fault (NAF). The geological record shows that this interaction between two strongly oblique components of boundary displacement started during Middle Miocene (Dewey and Şengör 1979; Şengör et al. 2005; Philippon et al. 2014), around 10 My before the NAF reached the Aegean (Armijo et al. 1999; Hubert-Ferrari et al. 2003; Şengör et al. 2005). On the other hand, the coeval extensional exhumation of high-pressure metamorphic rocks in the Cyclades and high-temperature metamorphic rocks in the Rhodope (Brun and Sokoutis 2007; Brun and Faccenna 2008) started in Middle Eocene (see review of data in Jolivet and Brun 2010 and Philippon et al. 2012). This brief summary of the extension history during a large part of the Tertiary indicates a process that has not been continuous, neither in time nor in space. This is illustrated by a striking difference in the distribution of Paleogene and Neogene sedimentary basins at Aegean scale (Fig. 2) suggesting that a major change in the dynamics of extension occurred in Middle Miocene, more 30 My after its onset.

The present article describes back-arc extension in the Aegean, in two main stages localized from Middle Eocene to Middle Miocene and distributed since Middle Miocene, and their most significant large-scale features in terms of sedimentation, deformation and metamorphism. Then, it presents a 3D restoration of the extensional displacements in four steps since Middle Eocene. It is shown that the transition in the mode of extension from localized (core complex) to distributed (wide rift), during Middle Miocene, is coeval with an acceleration of trench retreat. Finally, it is argued that this acceleration i) likely resulted from the tearing of the Hellenic slab documented by mantle tomography and ii) was coeval with the onset of Anatolia westward displacement.

Stage 1: Paleogene basins and ductile exhumation of metamorphic rocks

The first stage of extension, from Middle Eocene to Middle Miocene is recorded in the deposition of sedimentary basins and in the exhumation of high-temperature metamorphic core complexes and high-pressure metamorphic belts.

Paleogene basins that mostly contain Middle Eocene and/or Oligocene sediments are located i) on top of the Rhodopia block (Trace Basin: Görür and Okay 1996; Siyako and Huvaz 2007; Kilias et al. 2013); Vardar-Thermaikos Basin: Roussos 1994; Carras and Georgala 1998) and ii) on top of Pelagonia (Mesohellenic Trough: Doutsos et al. 1994; Ferrière et al. 2004) (Fig. 2a). The Thrace Basin that started subsiding in Early Eocene contains sedimentary rocks from Lower-Middle Eocene to Pleistocene, reaching a thickness up to 9000 m. The sedimentary units are dominantly marine-prodelta organic-rich shales and turbidites. The transition from Eocene to Lower Oligocene outcrops in the Lemnos Island (Maravelis and Zelilidis 2011). The Thrace Basin has recorded only moderate tectonic events. The initial subsidence controlled the deposition of Middle-Eocene to Oligocene sediments. Early Miocene sediments deposited during an event of inversion/folding are unconformably sealed by Middle to Late Miocene deposits. The Mesohellenic Through (MHT) extends over 300 Km with a mean width of 40 km from Albania to Greece along a NNW-SSE trend along the northern side of the Pindos suture zone (Doutsos et al. 1994; Ferrière et al. 2004). Its sedimentary fill also ranges from the Late Eocene to Middle Miocene. A first megasequence is composed, from base to top, of Late Eocene tectonic breccia, mass transport deposits, turbidites, fluvial conglomerates and deltaic plain sediments at the transition with the Oligocene. A second megasequence is characterized by Oligocene carbonates at the base. This platform is rapidly drowned by a rapid subsidence with the deposition of hundred meters of sands and silts organized in deltaic lobes.

The *Southern Rhodope Core Complex* (SRCC) (Fig. 3) (Dinter and Royden 1993; Sokoutis et al. 1993; Brun and Sokoutis 2007), located to the North of the Vardar suture zone, started to develop in Middle Eocene, around 45 Ma, and was controlled by the SW dipping Kerdylion detachment. The detachment hanging-wall is made of the metamorphic units of the Chalkidiki peninsula whose tectonic-metamorphic evolution is dominantly Mesozoic and which correspond to the western and most external part of Rhodopia (Kydonakis et al. 2015*b* and in press). The detachment footwall (i.e. the core) consists mostly a Hercynian basement made of orthogneisses, paragneisses and marbles dated as Permian at their base (i.e. a Pelagonian-type assemblage) affected by a high-temperature metamorphism that at many places reached partial melting in Barrovian-type metamorphic conditions (Dimitriadis 1989). To the North, the Nestos Thrust (Burg 2011; Nagel et al. 2011) separates these core units from the northern part of Rhodopia. Therefore, at regional-scale, the SRCC corresponds to a tectonic window in which Pelagonia is exposed. Consequently, we interpret the Nestos thrust that separates northern Rhodopia from Pelagonia as the Vardar Suture Zone. Prior to the 50 Ma migmatisation (Wawrzenitz and Krohe 1998), the Pelagonian core units were sheared and duplicated by SW directed thrusting (Brun and Sokoutis 2007). From Middle Eocene to Middle Miocene, the same units, as well as Oligocene and Lower Miocene granite intrusions (Kyriakopoulos et al. 1989, 1997; Kolocotroni and Dixon 1991; Dinter et al. 1995), recorded a second shearing event again toward the SW but in extension, during the exhumation of the core complex (Dinter and Royden 1993; Sokoutis et al. 1993); that extensional phase was primarily controlled by the SW-dipping Kerdylion Detachment (Brun and Sokoutis 2007). Everywhere within the exhumed units, the gneisses are mylonitic but approaching the Kerdylion Detachment they become ultramylonitic with thick cataclasites at the hanging-wall contact. Paleomagnetic data (Dimitriadis et al. 1998) indicate that the core complex exhumed during a 30° dextral rotation of the hanging-wall (Chalkidiki Peninsula) what is in agreement with the northwestward-closing triangular shape of the core complex map contours at regional scale (Brun and Sokoutis 2007). Since Middle Miocene, the exhumed core units have been segmented by two sets of normal faults trending NE-SW and NW-SE that controlled the deposition of Neogene basins (Lalechos 1986; Snel et al. 2006, Brun and Sokoutis 2007). In its largest width, to the Southeast, the bulk extensional displacement, including the brittle segmentation of the core complex, reached around 120 km. The *Central Cyclades Core Complex* (CCCC) (Philippon et al. 2012) is located the South of the Vardar Suture Zone and outcrops in the central islands of the Cyclades (Fig.3): Naxos-Paros and Mykonos-Delos-Rhenia. This core complex developed entirely within the Adria crustal block. The core units display a high-temperature metamorphism reaching partial melting that was superposed to a previous stage of high-pressure metamorphism. In Paros a fast heating from 350°C to 700°C occurred between 35 and 20 Ma (Bargnesi et al. 2013). In Naxos, where the peak of high-pressure metamorphism is dated around 45-50 Ma (Duchene et al 2006; Martin et al 2006), partial melting commenced prior to 20.7 Ma (Keay et al. 2001). A characteristic PTt trajectory of Naxos migmatites is shown in Figure 3 (modified after Duchêne et al. 2006). Core units show a stretching lineation dominantly oriented N-S with an associated top N sense of shear in Naxos-Paros (Gautier et al. 1989, 1993; Urai et al. 1990; Buik 1991) and NE-SW-oriented with a top NE sense of shear in Mykonos-Delos-Rhenia (Leconte et al. 2010) in agreement with a N-dipping but wavy detachment in Naxos-Paros and a NE-dipping detachment in Mykonos-Delos-Rhenia. These differences in structural and kinematic patterns are often interpreted as two separated core complexes with independent and non-connected detachments (e.g. Jolivet et al. 2010; Denèle et al. 2011). Consequently, this would imply distinct dynamics of development. The two groups of islands are separated by a regional-scale discontinuity trending NE-SW (Gautier and Brun 1994; later called "Mid-Cyclades Lineament" by Walcott and White 1998). Philippon et al. (2012) showed that the restoration of post-Middle Miocene faulting using available paleomagnetic data brings the two trends of stretching lineations into parallelism and the two groups of islands in geometrical continuity, revealing that hidden below the scattering of islands was initially a single core complex (i.e. the CCCC). The restoration also showed that the Mid-Cyclades Lineament can be interpreted as a dextral strike-slip fault, with an offset in the order of 50 km, that was called by Philippon et al. (2014) Myrthes–Ikaria fault (MIF in Fig. 3) as it transforms the post-Middle Miocene opening of the Myrthes and Ikaria basins located at its SW and NE tips, respectively. In this frame, the wavy shape of the Naxos-Paros detachment appears to result from an E-W component of shortening (as already suggested by Avigad et al. 2001 at the scale of the central Cyclades and by Urai et al. 1990 and Buik (1991) from the observation of outcrop-scale folds in Naxos).

High-pressure metamorphism (In blue in Fig. 4) affected Adria and partly Pelagonia during the closure of the Vardar and Pindos oceanic domains. Their exhumation was accommodated by extension, dominantly during “Stage 1” and partly during “Stage 2”. The Cycladic Blueschist Unit (CBU) is constituted by: i) at the base, a Hercynian basement dominantly made of granite orthogneisses, ii) a sedimentary cover where alternate marbles and schist sequences whose depositional ages range from Visean to Eocene and iii) at the top, an ophiolitic mélange made of serpentine schists with Triassic to Cretaceous metagabbro and metabasalt knockers that could represent either relicts of the Pindos Ocean itself or part of the Adria subcontinental lithospheric mantle that was partially molten during the stretching and rifting stage of the Pindos ocean. The rather similar ranges of pressure peaks in the oceanic-type rocks (0.8–2.2 GPa) and in the sedimentary cover (0.6–1.8 GPa) indicate that the basement, its sedimentary cover and the oceanic-type rocks were subducted at comparable depths. The compilation of geochronological data obtained by various methods in 10 different Cycladic islands (Fig.5 in Philippon et al. 2012) shows: i) that the ages of high-pressure metamorphism range between 58 and 40 Ma and ii) that the blueschist-greenschist transition occurred in a narrow age range of 3 My between 35 and 32 Ma. This indicates that the CBU was exhuming in Late Eocene-Early Oligocene as a whole coherent unit, in agreement with the preservation, in many islands, of the superposition cover on basement with or without ophiolitic mélange at the top. In addition, nummulitic turbidites (Lutetian) are involved in thrust deformation and have recorded a metamorphic pressure of 1–1.2 GPa (Shaked et al. 2000; Ring et al. 2007; Rosenbaum and Ring 2007). Together with the Middle Eocene age of the youngest pressure peaks, this shows that subduction-related thrusting was active until Middle Eocene. As the blueschist-greenschist transition occurred between 35 and 32 Ma, the delay between the end of subduction and the onset of exhumation has been short, more likely less than 5 My. The PTt trajectory of Tinos blueschists (Fig. 4) (Parra et al 2002; Jolivet and

Brun 2010) shows that an isobaric heating occurred during exhumation between 37 and 33 Ma. As Tinos is close to the CCCC (Fig. 3) this is more likely related with the heating observed in Paros in the same range of ages (Bargnesi et al 2013). Three main events of pervasive ductile deformation that can be characterized at regional scale by stretching lineations and associated senses of shear characterize the CBU (Philippon et al. 2012): (1) prior to at least 40 Ma, a subduction-related layer-parallel shear top to SW and top to S to the NW and to the SE of the MIF, respectively (Black arrows in Fig. 4), (2) from 40 to 20 Ma, an exhumation-related layer-parallel shear of weak to moderate intensity, prior to the onset of the North Cycladic detachment, top to N or NE to the NW and to the SE of the MIF, respectively (White arrows in Fig. 4), (3) from 20 to 13 Ma and observed in the islands adjacent to the North Cycladic detachment, a top to NE shear in general of strong intensity affects the blueschists as well as high temperature rocks of the CCCC (Red arrows in Fig. 3). The *high-pressure metamorphic unit of Peloponnese and Crete* is characterized by an exhumation history younger than the CBU one (Fig. 4). It was still undergoing burial when the CBU was already exhuming. Exhumation occurred in Late Oligocene-Lower Miocene without significant heating during exhumation. In this most external part of Adria, high-pressure low-temperature (HP-LT) metamorphism is only recorded in the " Phyllite–Quartzite Nappe " (PQN) (see comprehensive review by Jolivet et al. 2010*b* and references therein). The HP-LT PQN is sandwiched between two thick thrust units composed of Triassic to Eocene formations, namely the Gavrovo–Tripolitza Nappe (GTN) on top and the "Plattenkalk Nappe" below. As pointed out by Stöckhert et al. (1999), the average resistance of the PQN was much smaller than the overlying and underlying units and consequently localized a large part of the deformation during burial and exhumation. From a mechanical point of view, the PQN is therefore a décollement (i.e. dominated by layer-parallel shear) and relating its deformation to a detachment (shear zone cutting down section), as done in most published works, is rather misleading. This is confirmed by the presence of the GTN over the whole Peloponnese-Crete region and the common outcropping of the PQN in windows of the GTN. A detachment, significant at regional-scale, should have exposed the PQN over a large domain without the GTN on top. In Peloponnese, stretching lineations related to thrusting and exhumation trend EW but with a sense of shear top to W for thrusting (black arrows in Fig. 4) and top to E for exhumation (white arrows in Fig. 4). In Crete, stretching lineations related to exhumation trend NS (white arrows in Fig. 4). The orthogonality of stretching directions related to exhumation and the convergence of associated senses of shear imply that Peloponnese and Crete have undergone a nearly 90° relative rotation after the end of ductile deformation.

In summary, the exhumation of core complexes (high-temperature metamorphism) and blueschists (high-pressure metamorphism) results from significantly different mechanisms of development, primarily controlled by temperature-dependent rheology of the crustal units. Therefore, their location in the Aegean, as well as their relative timing of development, has an important mechanical significance:

- The SRCC started to develop in Middle-Late Eocene in North Aegean when the CBU started to exhume in central Aegean,
- The CCCC developed in central Aegean in lower Miocene almost synchronous with the onset of HP-LT PQN exhumation in Peloponnese and Crete.
- The sense of shear and detachment dip in core complexes and sense of shear in high-pressure rocks, is top to SW in North Aegean (SRCC), to NE in central Aegean (CBU and CCCC) and to E and N in South Aegean (HP-LT PQN).
- The part of exhumation synchronous with ductile deformation ended in Middle Miocene in all types of metamorphic rocks, either high-temperature (SRCC and CCCC) or high pressure (CBU and HP-LT PQN) and whatever age of onset.

Remark: The high-pressure to ultrahigh-pressure metamorphic units of the Southwest Rhodope (Kydonakis et al. 2015*b*) and the North Rhodope (Mposkos and Kostopoulos 2001, Liati 2005) developed during the Cretaceous, and were exhumed before Eocene, prior to the onset of back-arc extension in the Aegean (Kydonakis et al. 2014, Kydonakis et al. 2015b and 2015c) controlled by the Hellenic slab rollback. Therefore, they are outside the scope of the present paper.

Stage 2: Neogene basins, segmentation of metamorphic units and dextral transtensional faulting

The *Neogene basins* (Fig. 2b) whose deposition started in Middle Miocene constitute one of the most striking geological features of the Aegean domain, both onshore and offshore. They emplaced on all types of rock units (Paleogene basins, high-temperature or high-pressure metamorphic units, plutonic massives and volcanic buildups) of Rhodopia, Pelagonia and Adria and over around 1000 km from Crete to Rhodope. The earlier deposits are Langhian-Serravalian in some basins of the North Aegean (e.g. Prinos; Chiotis 1984; Beniest et al. 2015). Where structural data are available, field measurements or seismics, tectonic setting of most basins is extensional or transtensional (e.g. Mercier et al. 1987, 1989; Lyberis 1984; Mascle and Martin 1990; Koukouvelas and Aydin 2002; Sakellariou et al. 2013). In the islands of the North Aegean and Eastern Cyclades where it can be observed, the Late Miocene corresponds to continental lacustrine and alluvial series (Lesbos and Chios: Jones 1971; Samos: Weidmann et al. 1984, Beniest et al 2015). In Samos, the sediments are dated from 10 to 6 Ma by the intercalation of volcanic rocks (Weidmann et al. 1984) and mammals (Koufos et al. 2009), with a very rapid subsidence until 8 Ma (Deschamps et al. 2013). During the Messinian, a sea of brackish-water character developed between the Paratethys to the North and the Mediterranean to the South. At that time the Aegean Sea was principally fed by surrounding rivers and/or by Paratethyan waters. The sedimentary sequence deposited is principally composed of limestone containing brackish-water Paratethyan fauna, with some intercalations with Mediterranean species indicating the re-establishment of a non-permanent Atlantic–Mediterranean connection and, thus, replenishment of marine waters (Bache et al 2011). The Pliocene-Quaternary is characterized by a definitive restoration of the marine conditions in the Aegean.

Low-temperature thermochronology ages, obtained by various methods (apatite and zircon fission-track and U-Th/He on apatite and zircon) in high-temperature and high-pressure metamorphic units, which were exhumed during the first stage of extension, are dominantly Serravalian-Tortonian, over the whole Aegean (Fig. 5). This indicates that metamorphic rocks of the SRCC, the CBU-CCCC and Peloponnese-Crete, whose onsets of exhumation were different, were reaching the surface in Middle-Late Miocene. In the core complexes and high-pressure metamorphic rocks of the Aegean these ages of exhumation are commonly considered to provide an age for the end of normal sense displacement along a detachment. But the synchronism, at the whole Aegean scale, between the first sediment deposition in Neogene basins and the final stages of metamorphic rock exhumation put this type of interpretation in question, as most Neogene basins cannot be put in relation with any major crustal-scale detachment. In the Rhodope, Serravalian-Tortonian sediments are deposited on the hanging-wall of normal faults that cut through the metamorphic rocks of the SRCC (Brun and Sokoutis 2007). Simultaneously, the footwall of these faults was uplifted, reaching altitudes up to 1000-2000m. These normal faults trend either NW-SE, almost parallel to the core complex detachment, or NE-SW, perpendicular to the detachment. Whatever the fault trend, rocks from their footwall give the same range of thermochronology ages (Fig. 5), showing that these ages are not related to the functioning of the core complex detachment but to a superposed event of faulting that segmented the core complex. The

Cyclades archipelago resulted from the segmentation by normal faults within the CBU and the CCCC (see restoration in Philippon et al. 2012). As quoted in section 2.2, the Myrthes-Ikaria fault (MIF), which trends NE-SW, separated the Cyclades in two main domains (Fig. 6) (Philippon et al. 2014). To the NW of the MIF, the islands correspond to the residual reliefs remaining above the sea level from the uplift of normal fault footwalls. To the SE border of MIF, the high altitude of Paros-Naxos (up to 600 m) is likely related to upright folding of the core complex under a component of EW shortening (Avigad et al. 2001; Philippon et al. 2012). Two reasons could explain the lack of Middle-Late Miocene basin remnants in the Cyclades: i) the islands represent the upper part of normal fault footwalls and ii) erosion could have removed possibly inverted basins. However, Samos to the East of the Cyclades shows Tortonian sediments that were deposited in transtension and locally reworked in compression around 9 Ma (Ring and Ochrusk 2007). The statistical distribution of thermochronology ages (Fig. 5) obtained in 10 Cyclades islands, in either the CBU or the CCCC, is Middle-Late Miocene with a strong peak in Tortonian (See data compilation in Fig.12 of Philippon et al. 2012).

Dextral strike-slip faulting is an important part of the active Aegean fault pattern, in particular in the North Aegean, recognized through dynamic analysis of fault systems (Mercier et al 1987, 1989; Lyberis 1984; Lyberis and Sauvage 1985), structural mapping (Armijo et al. 1999; Papanikolaou et al. 2006), seismicity and earthquake focal mechanisms (Hatzfeld 1999; Taymaz et al. 1991; Goldworthy et al. 2002). Among these faults, the 1200 km-long *North Anatolian Fault* (NAF), which today accommodates the westward displacement of Anatolia, focus considerable and justified attention related to seismic risk from both societal consequences and scientific points of view. In the frame of this paper, our concern is the role, in time and space, that the NAF played in the Aegean dynamic evolution since Middle Miocene, called here stage 2 extension. Thirty-six years ago, Dewey and Şengör

(1979) recognized that the NAF had been preceded by a larger zone of displacement initiated in Late Miocene, connected to the Bitlis suture in eastern Anatolia, as the "Proto-Anatolian Transform". More recently, Şengör et al. (2005) on the basis of quantitative arguments, derived from the study of Neogene basins in North Anatolia, showed that the NAF resulted from strain localization within the 100 km wide North Anatolian Shear Zone (NASZ). Localization in Western Turkey (Dardanelle strait) is estimated around 5 Ma (Armijo et al. 1999). To the West of the Dardanelle Strait, the NAF takes a NE-SW direction and joins the SSW-NNE-trending North Aegean Through (NAT) (Lyberis et al. 1984; Koukouvelas and Aydin 2002) that is the major bathymetric depression of North Aegean (Papanikolaou et al. 2002). The NAT likely originated in Paleogene as a transtensional structure to laterally accommodate the dextral rotation of the Chalkidiki block with reference to North Rhodope during the exhumation of the Southern Rhodope Core Complex. In the junction area between the NAT and the NAF, positive flower structures (Roussos and Lyssimachou 1991) suggest a reactivation of pre-existing faults of the NAT at the propagating tip of the NAF. The dextral strike-slip displacements that characterize the NAF become transtensional in the NAT with a series of North-dipping normal faults oriented WNW-ESE that branch onto the sharp and linear eastern border of the NAT (Fig. 6). The superposition of the GPS displacement field on top of the map of Neogene basins (Fig.7) shows that the NAT separates two domains where displacements are southward and low rate (< 0.5 cm/y) to the North and southwestward and medium rates (> 2.1 cm/y) to the South. Syn-sedimentation rollover geometry of Neogene basins of Southern Rhodope indicates a NE-SW direction of stretching in Pliocene (Brun and Sokoutis 2007). Kinematic analysis of faults systems in North Aegean (Lyberis 1984; Lyberis and Sauvage 1985; Mercier et al. 1987, 1989) revealed that a change in the direction of stretching from NE-SW to N-S (Fig. 8) occurred in Lower Pleistocene. This suggests that the present-day displacement pattern became fully installed rather recently, in Lower-Middle

Pleistocene. A similar change in the direction of stretching from NE-SW to N-S is also observed in the Southern Hellenides during the Pliocene (See Fig. 3 in Papanikolaou and Royden 2007). Figure 6 shows that the *Myrthes-Ikaria fault* (MIF) is the offshore extend of the onshore *Ismir-Balikeshir transfer zone* (IBTZ) (Sozbilir et al. 2010; Ersoy et al. 2012; Uzel et al. 2013) (Fig. 6). Lower(?)-Upper Miocene sedimentary-volcanic basins were deposited in this transtensional corridor, located at the northwestern border of the Menderes Massif (Ersoy et al. 2012). Simultaneously, grabens developed in the Menderes, accommodating a NE-SW direction of stretching. Without entering here into the complexities of the paleomagnetic record of block rotations in IBTZ and Menderes (Uzel et al. 2015), it must be mentioned that dextral strike-slip shear in IBTZ accommodated a CCW rotation of the southern Menderes of around 30° (Pourteau et al. 2010; van Hinsbergen et al. 2010), likely comparable to the 33° CCW rotation of the Naxos-Paros block in the Cyclades (Morris and Anderson 1996) accommodated by dextral strike-slip offsets along the MIF (Philippon et al. 2012, 2014). Over 450 km, from Myrthes Basin to Balikeshir, this dextral strike-slip fault zone was active since Middle Miocene –i.e. around 10 My before the arrival of the NAF in the North Aegean. We lack of direct markers to identify when displacements ceased on this fault. We may hypothesize that it should be around 5 Ma when the NAF fully localized, reaching the western part of Marmara Sea This would be in agreement with the last exhumation ages recorded by low-temperature thermochronology (Fig. 5). The Myrthes-Balikeshir fault zone accommodated the difference in amount of stretching between the two domains that it separates. Therefore it is interesting to note that, in terms of displacement, the bulk 50 km offset of dextral strike-slip along the fault that was estimated in the central Cyclades (Philippon et al. 2014) is in rather good agreement with the 50 km of NE-SW trending extension estimated in the southern part of the Menderes Massif (van Hinsbergen, 2010).

In summary, the mode of extension during this second stage of back-arc extension is in strong contrast with the one that characterizes the first stage. Extension passed in Middle Miocene from the core complex mode to the wide rift mode (Buck 1991; Brun 1999), as demonstrated by the deposition of extensional or transtensional Neogene basins across the whole Aegean offshore and onshore. The interruption of ductile exhumation in Middle Miocene, in all types of metamorphic rocks (HT as well as HP) whatever their age of onset, as well as the segmentation of the metamorphic units and the deposition of Neogene basins on top of them suggest that the transition between the two modes of extension was not progressive and likely occurred in a rather short delay.

Restoration of 45 My of back-arc extension

Restorations of deformation in the shallow upper crust have demonstrated the difficulties and limitations inherent to this type of exercise. At lithosphere scale, like attempted here, restoration is face to more difficulties and depends even more than at smaller scales on the interpretation that is made, prior to restoration, of i) the tectonic setting in time and space of the domain to be restored and ii) the understanding of mechanical processes involved. In other words, such a restoration cannot be expected to put in evidence something that has not been identified and understood prior to restoration, whatever the particular techniques used for restoration. However, in spite of these limitations and in a case like the Aegean whose 3D evolution is rather complex, it is the best way: i) to test the coherence of the proposed interpretations, ii) to discuss their 3D implications, and iii) to make them more easily accessible and opened to critical assessment by anyone.

The 3D reconstruction of the 45 My history of back-arc extension presented in this section was carried out in two steps, in map view and then in cross-sections. It was performed manually using standard graphical techniques because a computer procedure appropriate for restoration at lithosphere scale does not exist yet. The two-step restoration, in map view and in cross-section, was performed at 5, 15 and 45 Ma for which enough geological and geophysical data were available to satisfactorily constrain a model. An intermediate model at 30 Ma was obtained by interpolation.

Restoration in map view was carried out using the data from references quoted in the two previous sections plus: i) Geological map of Greece at various scales (IGME), ii) offshore maps (synthesis by Mascle and Martin 1990), ii) paleomagnetic data (see compilations in: i) Kissel and Laj 1988 and Van Hinsbergen et al. 2005 at Aegean scale, ii) Dimitriadis et al. 1998 for northern Greece, Morris and Anderson 1996 for the Cyclades and Kissel et al. 1993 for Western Anatolia), iii) Principal directions of stretching and shear sense recorded in HT and HP metamorphic rocks during subduction (Black arrows) and extensional exhumation (White arrows) (Figs. 3 and 4). Colors of the restored maps are the same than those of the present-day map (Fig.1). The darker blue band in Adria corresponds to the external fold and thrust belt of the Pindos Nappe. All maps show the position of Black Sea and the location of the rotation pole of Scutary-Pec (Albania) (Kissel et al. 1995) around which the Southern Hellenides and western Cyclades rotated clockwise by 50° since Oligocene (Kissel and Laj 1988; Van Hinsbergen et al. 2005). The present restoration integrates more detailed restoration models dedicated to the Cyclades (Philippon et al. 2014) and to Northern continental Greece (Kydonakis et al. 2015*a*).

The series of maps (Fig. 9) shows: i) the change in geometry and location of the Vardar and Pindos suture zones, ii) the approximate position of the trench, iii) the development of major strike-slip faults, in particular the Myrthes-Ikaria Fault (MIF) between 15 and 5 Ma and the North Anatolia Fault (NAF) since 5 Ma and iv) the location of Paleogene basins (in orange). The present-day strong obliquity between stretching directions related to ductile exhumation in Peloponnese and Crete is almost entirely restored into a single NE-trending direction at 5Ma. At 15 Ma, the stretching directions of Peloponnese, Crete and Cyclades are all parallel and trending NNE with Crete located below the Cyclades. In northern Greece, the progressive exhumation of the Southern Rhodope Core Complex occurred during the deposition of the Thrace Basin (TB). The lateral transition between these two major geological features of the North Aegean was likely accommodated by sinistral transcurrent displacements along the North Aegean Trench (NAT), from 45 to 5 Ma. At 30 Ma, all the Paleogene basins (Mesohellenic Trough (MHT), North Aegean Trough (NAT), Xanthi Basin (XB) and Thrace Basin (TB)) are close to each other, forming a band slightly oblique to the trend of the suture zones of Vardar and Pindos. Our restoration is in a rather good agreement with the one of Royden and Papanikolaou (2011; their Fig. 15), up to lower Oligocene, but at strong variance with the one of van Hinsbergen and Schmid (2012; their Fig. 12) that requires a component of EW stretching across the whole Aegean accommodated by N-S or NE-SW trending extensional detachments, giving in the southern Aegean an arc-parallel extension up to 650 Km between 15 Ma and present (i.e. more EW displacement than the bulk amount of trench retreat). In addition, the van Hinsbergen and Schmid's model, contrary to our model, totally ignores the kinematics of HP-metamorphic rocks exhumation, as their model implied stretching directions trending perpendicular or strongly oblique to the stretching directions recorded in rocks.

Restoration in cross-section was done using the following input data: i) restored maps (previous section), ii) peak pressures recorded in high pressure metamorphic rocks (see review in Jolivet and Brun 2010 and Philippon et al. 2012), iii) present-day crustal thickness (Tirel et al. 2004) and iv) present-day geometry of the top slab surface from S-wave tomography (Salaün 2011). Two parallel sections oriented NE-SW have been restored: i) from NW Peloponnese to North Rhodope (Section A) and ii) from Southeast Peloponnese to the West of Marmara Sea (section B) (Fig. 10). The present-day geometry of the slab in section A shows a fold that passes laterally to a slab tear in section B. In section A, extension is mostly located to the North of the Vardar suture zone (Vardar-Thermaikos Gulf and SRCC). At 50 Ma, the Pelagonian crust that has been entirely subducted starts to delaminate from the underlying mantle allowing the asthenosphere to flow below the crust. As a consequence, fast and strong crustal heating, up to partial melting, strongly weakened the crust. At 45 Ma, after the subduction of the narrow Pindos oceanic domain, the Adria crust was dominantly subducted and core complex extension (SRCC) started at the back of the thrust wedge, controlled by the Kerdylion Detachment. At 15 Ma, core complex extension gave place to wide rift mode of extension with deposition of Neogene basins, the larger one being the Vardar-Thermaikos Gulf basin. Along this section, located to the West of the Corinth Gulf, trench retreat reached around 300 Km. Most of the extension was located in the North Aegean and, conversely, the Adria crust (Southern Hellenides) was only weakly extended. The section B shows the same sequence of tectonic events but with two major differences: i) trench retreat reached around 500 Km and extension affected the full Adria crustal block and ii) to the North, instead of a core complex, extension gave birth to the Thrace Basin on top of Rhodopia. The series of sections illustrates that the exhumation of high-pressure metamorphic rocks of Adria and partly Pelagonia occurred entirely in extension. Between 45 and 15 Ma, the whole initial thrust pile collapsed southward and both Pelagonia and Adria underwent a layer-parallel top to North sense of shear bringing them in a lower crustal depth. Since 15 Ma, the southern part of the extending thrust wedge that was located to the South of the slab tear, underwent a strong distributed extension that achieved the exhumation of metamorphic rocks up to surface.

Discussion: Dynamics of back-arc extension in the Aegean

Back-arc extension in the Aegean occurred in two main stages, first between Middle Eocene and Middle Miocene and second since Middle Miocene. The first stage, prior to Middle Miocene, is illustrated by the deposition of Paleogene basins (Fig. 2) and the simultaneous exhumation of high-temperature and high-pressure metamorphic rocks in a core complex northward and a blueschist belt southward. This occurred in two steps: i) In Middle Eocene (45 Ma) started the exhumation of the SRCC in the Rhodope (Fig. 3) and the CBU in the Cyclades (Fig. 4) and in Lower Miocene (around 23 Ma) the exhumation of the CCCC in the Cyclades (Fig. 3) and the PQN blueschists in Peloponnese and Crete (Fig. 4). During the second stage, since Middle Miocene, the HP and HT metamorphic units exhumed during the first stage were segmented dominantly in transtension, synchronous with Neogene basin deposition.

The restoration of displacements that is well constrained in continental Greece and central Aegean by numerous paleomagnetic data, kinematic indicators in metamorphic rocks and geochronological data shows that *an acceleration of trench retreat started in Middle Miocene* (Fig. 11). The rate of trench retreat that was rather low, around 0.6 cm.y^{-1}, during the first stage of extension increased to around 1.7 cm.y^{-1} between Middle Miocene and Pliocene to reach 3.2 cm.y^{-1} during the last 5 Ma. This is in agreement with the "dramatic acceleration" of back-arc extension deduced by Van Hinsbergen et al. (2010) from their study of the Menderes Massif in western Anatolia.

This acceleration of trench retreat (i.e. extensional boundary displacement), first by a factor 2 after Middle Miocene and then by a factor 5 after Pliocene, was likely responsible for the observed change in the mode of extension, from localized to distributed (i.e. from core complex to wide rift; Buck 1990; Brun 1999; Tirel et al. 2006, 2008; Gueydan et al. 2008; Kydonakis et al. 2015*a*). Mechanical modeling of the extension of a two-layer brittle-ductile system shows that an increase in strain rate increases the strength of the ductile layer and consequently the coupling between the brittle and ductile layers, giving a transition from localized to distributed extension (Brun 1999; Schueller et al. 2005, 2010).

In addition to this major change in the style of extension, it is interesting to note that the difference in P/T ratios between the high-pressure metamorphic rocks of Cyclades and Crete agrees well with an increase in the velocity of trench retreat (Gueydan et al. 2009).

The acceleration of trench retreat is probably related to a lateral tearing of the Hellenic slab below western Anatolia (Brun and Sokoutis 2010; Van Hinsbergen et al. 2010) identified by P-wave tomographic models of the upper mantle (Piromallo and Morelli 2003; Biryol et al. 2011). The improved resolution of mantle structure provided by S-wave tomographic modeling (Salaün et al. 2012) allowed a mapping of the slab tear with three main trends (Salaün 2011) (Fig. 10): WNW-ESE, below the central part of North Aegean Sea, and NNW-SSE and E-W almost parallel to the two mean coastline trends of Southwest Anatolia. Section B (Fig. 10) shows the geometry of the top slab below the North Aegean. Whereas the exact timing of slab tearing is difficult to constrain, the sudden change in the mode of extension that is associated with the acceleration of slab retreat strongly supports that slab tearing should have started to develop earlier, possibly in Early Miocene, to become fully efficient from 15 Ma onward.

The transtensional deformation pattern that results from the interaction between Hellenic trench retreat and Anatolia westward displacement and that is still active in the Aegean took place in Middle Miocene, showing that the westward displacement Anatolia was coeval with the acceleration of trench retreat. Whereas the North Anatolian fault plays a major role in the present-day kinematic pattern, *the Myrthes-Ikaria-IBTF was the first large dextral strike-slip fault zone to develop.* Its location close to the Izmir-Ankara suture zone and parallel to it suggests that the suture zone was acting as weak zone able to localize displacements at the onset of Anatolia westward displacement, as illustrated in the laboratory experiments of Philippon et al. (2014). However, this interaction between two plate boundary displacements raises a still opened fundamental issue: What is the dynamic relationship between slab tearing and Anatolia displacement? Which one controlled the development of the other?

Acknowledgements

J-P Brun thanks Ali Polat for inviting the paper. Research was financially supported by ANR EGEO (ANR-06-BLAN-0156) lead by L. Jolivet (J-PB, FG and MP), the European Union FP7 Marie Curie ITN “TOPOMOD” contract 264517, lead by C. Faccenna (J-PB, CF, FG, KK and DS) and by the Netherlands Research Centre for Integrated Solid Earth Science (DS). We thank the guest editor C. Şengör, D. Van Hinsbergen and an anonymous reviewer for their comments and suggestions of improvement.

References

Armijo, R., Meyer, B., Hubert, A., and Barka, A. 1999. Westward propagation of the north Anatolian into the northern Aegean: timing and kinematics. Geology, **27** : 267-270.

Avigad, D., Ziv, A., and Garfunkel, Z. 2001. Ductile and brittle shortening, extension-parallel folds and maintenance of crustal thickness in the central Aegean (Cyclades, Greece). Tectonics, **20** : 277-287. doi:10.1029/2000TC001190.

Bache, F., Popescu, S.-M., Rabineau, M., Gorini, C., Suc, J.-P., Clauzon, G., Olivet, J.-L., Rubino, J.-L., Melinte-Dobrinescu, M.C., Estrada, F., Londeix, L., Armijo, R., Meyer, B., Jolivet, L., Jouannic, G., Leroux, E., Aslanian, D., Baztan, J., Dos Reis, A.T., Mocochain, L., Dumurdžanov, N., Zagorchev, I., Lesić, V., Tomić, D., Cağatay, M.N., Brun, J.-P., Sokoutis, D., Ucarkus, G., and Cakir, Z. 2011. A two-step process for the reflooding of the Mediterranean after the Messinian salinity crisis. Basin Research, **23** : 1–29, doi: 10.1111/j.1365-2117.2011.00521.x

Bargnesi, E.A., Stockli, D.F., Neil Mancktelow, N., and Soukis, K. 2013. Miocene core complex development and coeval supradetachment basin evolution of Paros, Greece, insights from (U–Th)/He thermochronometry. Tectonophysics, **595-596** : 165-182.

Beniest, A., Brun, J.-P., Jeroen Smit, J., Deschamps, R., Hamon, Y., Crombez, V., and Gorini, C. 2015. Structure and seismic stratigraphy of deep Tertiary basins in the northern Aegean Sea. Geophysical Research Abstract, **17**, EGU2015-746.

Biryol, C.B., S.L., Zandt, G., and Özacar, A.A. 2011. Segmented African lithosphere beneath the Anatolian region inferred from teleseismic P-wave tomography. Geophysical Journal International, **184** : 1037-105.

Bourcart, M. J. 1919. Sur la présence du Priabonien dans la région SE Salonique, Comptes Rendus de l'Académie des Sciences, Paris, 855-856.

Brix, M.R., Stöckhert, B., Seidel, E., Theye, T., Thomson, S.N., and Küster, M. 2002.

Thermobarometric data from a fossil zircon partial annealing zone in high pressure–low temperature rocks of eastern and central Crete, Greece. Tectonophysics, **349** : 309–326.

Brun, J.-P. 1999. Narrow rifts versus wide rifts: Inferences for the mechanics of rifting from laboratory experiments. Philosophical Transactions of the Royal Society, London, Ser. A, **357** : 695– 712.

Brun, J.-P., and Faccenna, C. 2008. Exhumation of high-pressure rocks driven by slab rollback. Earth and Planetary Science Letters, **272** : 1–7. doi:10.1016/j.epsl.2008.02.038

Brun, J.-P., and Sokoutis, D. 2007. Kinematics of the Southern Rhodope Core Complex (north Greece). International Journal of Earth Sciences, **96** : 1079–1099.

Brun, J.-P., and Sokoutis, D. 2010. 45 m.y. of Aegean crust and mantle flow driven by trench retreat. Geology, **38** : 815–818. doi: 10.1130/G30950.1.

Buck, W.R. 1991. Modes of continental lithospheric extension, Journal of Geophysical Research, **96** : 20161 - 20178.

Buick, I.S. 1991. Mylonite fabric development on Naxos, Greece. Journal of Structural Geology, **13** : 643–655.

Burg, J.-P. 2011. Rhodope: From Mesozoic convergence to Cenozoic extension. Review of petro-structural data in the geochronological frame. In: (Eds.) Emmanuel Skourtsos and Gordon S. Lister, Journal of the Virtual Explorer, **39** : paper 1. doi:10.3809/jvirtex. 2011.00270

Carbotte, S.M., Arko, R., Chayes, D.N., Haxby, W., Lehnert, K., O'Hara, S., Ryan, W.B.F., Weissel, R.A., Shipley, T., Gahagan, L., Johnson, K., and Shank, T. 2004. New integrated Data Management System for Ridge 2000 and MARGINS Research, Eos Transactions. AGU, **85**, 51, 553, doi : 10.1029/2004EO510002.

Carras, N., and Georgala, D. 1998. Upper Jurassic to Lower Cretaceous Carbonate Facies of African Affinities in a Peri-European Area: Chalkidiki Peninsula, Greece, Facies, **38** : 153-

164.

Channell, J.E.T., and Kozur, H. 1997. How many oceans? Meliata, Vardar, and Pindos oceans in Mesozoic Alpine paleogeography. Geology, **25** : 183–186.

Denèle, Y., Lecomte, E., Jolivet, L., Lacombe, O., Labrousse, L., Huet, B., and Le Pourhiet, L. 2011. Granite intrusion in a metamorphic core complex: the example of the Mykonos laccolith (Cyclades, Greece). Tectonophysics, **501** : 52–70. http://dx.doi.org/10.1016/j.tecto.2011.01.013.

Chiotis, E.D. 1984 . A Middle Miocene thermal event in northern Greece confirmed by coalification measurements. In : Dixon, J.E. and Robertson, A.H.F. (Eds) The Geological Evolution of the Eastern Mediterranean. Geological Society, London, Special Publications, **17** : 815-818. doi:10.1144/GSL.SP.1984.017.01.66.

Dercourt, J., Ricou, L.E., and Vrielynck, B. 1993. Atlas Tethys Paleoenvironmental Maps, Beicip–Franlab. Deschamps, R., Hamon, Y., Darre, T., Gorini, C., 2013. Caractérisation des séries lacustres du Miocène Supérieur de l'Ile de Samos. Un exemple de paléolac alcalin et salin, in: 14eme Congrès Français de Sédimentologie, Paris (Ed. ASF), **73** : 118.

Dewey, J. F., and Şengör, A. C. 1979. Aegean and surrounding regions: complex multiplate and continuum tectonics in a convergent zone. Geological Society of America Bulletin, **90** : 84-92.

Dimitriadis, S. 1989. Sillimanite grade metamorphism in the Thassos Island, Rhodope Massif, Greece, and its regional significance. Geologica Rhodopica, **1** : 190–201

Dimitriadis, S., Kondopoulou, D., and Atzemoglou, A. 1998. Dextral rotation and tectonomagmatic evolution of the southern Rhodope and adjacent regions (Greece). Tectonophysics, **299** : 159–173

Dinter, D.A., and Royden, L. 1993. Late Cenozoic extension in northeastern Greece: Strymon Valley detachment system and Rhodope metamorphic core complex. Geology, **21** : 45–48

Dinter, D.A., Macfarlane, A., Hames, W., Isachsen C., Bowring, S., and Royden, L. 1995. U–Pb and Ar/Ar geochronology of the Symvolon granodiorite: Implications for the thermal and structural evolution of the Rhodope metamorphic core complex, northeastern Greece. Tectonics, **14** : 886–908

Doutsos, T., Koukouvelas, I., Zelilidis, A., and Kontopoulos, N. 1994. Intracontinental wedging and post-orogenic collapse in Mesohellenic trough. – Geologische Rundschau, **83** : 257-275.

Duchêne, S., Aïssa, R., and Vanderhaeghe, O. 2006. Pressure–temperature–time evolution of metamorphic rocks from Naxos (Cyclades, Greece): constraints from Thermobarometry and Rb/Sr dating. Geodynamica Acta, **19** : 299–319.

Ersoy, E.Y., Helvaci, C., Uysal, I., Karaoğlu, Ö., Palmer, M.R., and Dindi, F. 2012. Petrogenesis of the Miocene volcanism along the Izmir–Balıkesir Transfer Zone in western Anatolia, Turkey: implications for origin and evolution of potassic volcanism in postcollisional areas. Journal of Volcanology and Geothermal Research, **241–242** : 21–38.

Faccenna, C., Jolivet, L., Piromallo, C., and Morelli, A. 2003. Subduction and the depth of convection in the Mediterranean mantle. Journal of Geophysical Research, **108** : 2099. http://dx.doi.org/10.1029/2001JB001690.

Faccenna C., Becker T.W., Auer L., Billi A., Boschi L., Brun J.-P., Capitanio F.A., Funiciello F., Horvàth F., Jolivet L., Piromallo C., Royden L., Rossetti F., and Serpelloni E. 2014. Mantle dynamics in the Mediterranean. Review of Geophysics, doi: 10.1002/2013RG000444

Ferrière, J., Reynaud, J.-Y., Pavlopoulos, A., Bonneau, M., Migiros. G., Chanier F., Proust, J.-N., and Gardin, S. 2004. Geologic evolution and geodynamic controls of the Tertiary intramontane piggyback Meso-Hellenic basin, Greece. Bulletin de la Société Géologique de France, **175** : 361-381.

Gautier, P., and Brun, J.-P. 1994. Crustal-scale geometry and kinematics of late-orogenic extension in the central Aegean (Cyclades and Evvia Island). Tectonophysics, **238** : 399–424.

Gautier, P., Ballèvre, M., Brun J.-P. and Jolivet, L. 1990. Cinématique de l'extension ductile à Naxos et Paros (Cyclades). C.R. Acad. Sci., Paris, **310** : 147-153.

Gautier, P., Brun, J.-P., and Jolivet, L., 1993. Structure and kinematics of Upper Cenozoic extensional detachment on Naxos and Paros (Cyclades Islands, Greece). Tectonics, **12** : 1180-1194.

Goldsworthy, M., Jackson, J., and Haines, J. 2002. The continuity of active fault systems in Greece. Geophysical Journal International, **148** : 596–618.

Görür, N., and Okay, A.I. 1996. A fore-arc origin for the Thrace Basin, NW Turkey. Geologische Rundschau. **85** : 662–668.

Gueydan, F., C. Morency, and J.P. Brun, 2008. Continental rifting as a function of lithosphere mantle strength, Tectonophysics, **460** : 83-93.

Gueydan, F., Le Garzic, E. and Carry, N., 2009. P/T ratio in high-pressure rocks as a function of dip and velocity of continental subduction. Lithosphere, **1** : 282-290.

Hatzfeld, D. 1999. The present-day tectonics of the Aegean as deduced from seismicity. In: Durand, B., Jolivet, L., Horvath, F & Séranne, M. (eds) The Mediterranean Basins: Tertiary Extension within the Alpine Orogen. Geological Society, London, Special Publications, **156** : 415-426.

Hollenstein, C., Müller, M.D., Geiger, A., Kahle, and H.-G. 2008. Crustal motion and deformation in Greece from a decade of GPS measurements, 1993–2003. Tectonophysics, **449** : 17–40, http://dx.doi.org/10.1016/j.tecto.2007.12.006.

Hubert-Ferrari, A., King, G., Manighetti, I., Armijo, R., Meyer, B., and Tapponnier, P. 2003.

Long-term Elasticity in the Continental Lithosphere; Modelling the Aden Ridge Propagation and the Anatolian Extrusion Process. Geophysical Journal International, **153** : 111-132.

Huet, B., Labrousse, L., and Jolivet, L. 2009. Thrust or detachment? Exhumation processes in the Aegean: Insight from a field study on Ios (Cyclades, Greece). Tectonics, **28** , TC3007, doi:10.1029/2008TC002397.

Jolivet, L., and Brun, J.-P. 2010. Cenozoic geodynamic evolution of the Aegean. International Journal of Earth Sciences, **99** : 109-138. doi:10.1007/s00531-008-0366-4.

Jolivet, L., and Faccenna, C. 2000. Mediterranean extension and the Africa–Eurasia collision. Tectonics, **19** : 1095–1106.

Jolivet, L., Trotet, F., Monié, P., Vidal, O., Goffé, B., Labrousse, L., Agard, P., and Ghorbal, B. 2010a Along-strike variations of P–T conditions in accretionary wedges and syn-orogenic extension, the HP–LT Phyllite–Quartzite Nappe in Crete and the Peloponnese. Tectonophysics, **480** : 133-148. doi:10.1016/j.tecto.2009.10.002.

Jolivet, L., Lecomte, E., Huet, B., Denèle, Y., Lacombe, O., Labrousse, L., Le Pourhiet, L., and Mehl, C. 2010b. The North Cycladic detachment system. Earth and Planetary Science Letters, **289** : 87–104. http://dx.doi.org/10.1016/j.epsl.2009.10.032.

Jolivet, L., Faccenna, C., Huet, B., Labrousse, L., Le Pourhiet, L., Lacombe, O., Lecomte, E., Burov, E., Denèle, Y., Brun, J.-P., Philippon, M., Paul, A., Salaün, G., Karabulut, H., Piromallo, C., Monié, P., Gueydan, F., Okay, A.I., Oberhänsli, R., Pourteau, A., Augier, R., Gadenne, L., and Driussi, O. 2013. Aegean tectonics: Strain localisation, slab tearing and trench retreat. Tectonophysics, **597** : 1-33. doi:10.1016/j.tecto.2012.06.011

Jones, K.D. 1971. An outline of the geology of the islands of Mytilini and Chios - in: Campbell, A.S. (ed.) - Geology and history of Turkey – Petroleum Exploration Society of Libya, Tripoli: 275-282.

Keay, S., Lister, G., and Buick, I. 2001. The timing of partial melting, Barrovian metamorphism and granite intrusion in the Naxos metamorphic core complex, Cyclades, Aegean Sea, Greece. Tectonophysics, **342** : 275– 312.

Kilias, A., Falalakis, G., Sfeikos, A., Papadimitriou, E., Vamvaka, A., and Gkarlaouni, C. 2013. The Thrace basin in the Rhodope province of NE Greece — A tertiary supradetachment basin and its geodynamic implications. Tectonophysics, **595–596** : 90–105.

Kissel, C., and Laj, C., 1988. The Tertiary geodynamic evolution of the Aegean arc: a paleomagnetic reconstruction. Tectonophysics, **146** : 183–201.

Kissel, C., Averbuch, O., Frizon de Lamotte, D., Monod, O., and Allerton, S., 1993. Preliminary paleomagnetic evidence of a post-Eocene clockwise rotation of the Western Taurides thrust belt, east of the Isparta reentrant (Southern Turkey). Earth and Planetary Science Letters. **117** : 1 – 14.

Kissel, C., Speranza, F., and Milicevic, V. 1995. Paleomagnetism of external southern Dinarides and northern Albanides: implications for the Cenozoic activity of the Scutari–Pec shear zone. Journal of Geophysical Research, **100** : 14999–15007.

Kolocotroni, C., and Dixon, J. 1991. The origin and emplacement of the Vrondou granite, Serres, NE Greece. Bulletin of the Geological Society of Greece, **25** : 469–483.

Koufos, G.D., Kostopoulos, D.S., and Vlachou, Th.D. 2009. The Late Miocene Mammal Faunas of the Mytilinii Basin, Samos Island, Greece: New Collection. 16. Biochronology. — Beiträge zur Paläontologie, **31** : 397–408.

Koukouvelas, I.K., and Aydin, A. 2002. fault structure and related basins of the North Aegean Sea and its surroundings. Tectonics, **21** : 1046. http://dx.doi.org/10.1029/ 2001TC901037.

Kydonakis, K., Gallagher, K., Brun J.P., Jolivet, M., Gueydan, F. and Kostopoulos, D. 2014. Upper Cretaceous exhumation of the western Rhodope Metamorphic Province (Chalkidiki

Peninsula, northern Greece), Tectonics, **33**, doi:10.1002/2014TC003572.

Kydonakis, K., Brun, J.-P., and Sokoutis, D. 2015a. North Aegean core complexes, the gravity spreading of a thrust wedge. Journal of Geophysical Research, Solid Earth, **120**, doi:10.1002/2014JB011601.

Kydonakis, K., Brun, J.-P., Sokoutis, D. and Gueydan, F. 2015b. Kinematics of Cretaceous subduction and exhumation in the western Rhodope (Chalkidiki block). Tectonophysics, **665** : 218–235

Kydonakis, K., Moulas, E., Chatzitheodoridis, E., Brun, J.-P**.** and Kostopoulos, D. 2015c. First-report on Mesozoic eclogite-facies metamorphism preceding Barrovian overprint from the western Rhodope (Chalkidiki, northern Greece). Lithos, **220–223** : 147–163. http://dx.doi.org/10.1016/j.lithos.2015.02.007

Kyriakopoulos, K., Pezzino, A., and Moro, A.D. 1989. Rb–Sr geochronological, petrological and structural study of the Kavala plutonic complex (N. Greece). Bulletin of the Geological Society of Greece, **XXIII** : 545–560

Kyriakopoulos, K.G., Magganas, A.C., Norelli, P., Bigazzi., G., Moro, A.D., and Kokkinakis, A. 1997. Thermochronological evolution of Symvolon and Pangeon pluton and their country rocks, Kavala area, N. Greece: an apatite fission track analysis, Neues Jahrbuch für Mineralogie , **H11** : 519 - 529.

Lalechos, N. 1986. Correlations and observations in molassic sediments in onshore and offshore areas of northern Greece. Lithos, **56** : 89–99

Lecomte, E., Jolivet, L., Lacombe, O., Denèle, Y., Labrousse, L., and Le Pourhiet, L. 2010. Geometry and kinematics of a low-angle normal fault on Mykonos island (Cyclades, Greece): evidence for slip at shallow dip. Tectonics, **29**, TC5012. http://dx.doi.org/ 10.1029/2009TC002564.

Le Pichon, X., and Angelier, J. 1981. The Aegean Sea. Philos. Philosophical Transactions of the Royal Society, London, Ser. **A 300** : 357– 372.

Liati, A., 2005. Identification of repeated Alpine (ultra) high-pressure metamorphic events by U–Pb SHRIMP geochronology and REE geochemistry of zircon: the Rhodope zone of Northern Greece. Contribution to Mineralogy and Petrology, **150** : 608–630

Lyberis, N. 1984. Tectonic evolution of the North Aegean trough, Geological Society, London, Special Publications, **17** : 709-725.

Lyberis, N., and Sauvage, J. 1985. Tectonic evolution of the North Aegean area during the Plio-Pleistocene. Bulletin de la Société Géologique de France, **I** : 581–595.

Maravelis, A., and A Zelilidis, A. 2011. Organic geochemical characteristics of the late Eocene-early Oligocene submarine fans and shelf deposits on Lemnos Island, NE Greece. Journal of Petroleum Science and Engineering, **71** : 160-168.

Marsellos, A.E., Min, K., and Foster David, A. 2014. Rapid Exhumation of High-Pressure Metamorphic Rocks in Kythera-Peloponnese (Greece) Revealed by Apatite (U-Th)/He Thermochronology. The Journal of Geology, **122** : 381–396.

Mascle, J., and Martin, L. 1990. Shallow structure and recent evolution of the Aegean Sea: A synthesis based on continuous reflection profiles. Marine Geology, **94** : 271–299. doi: 10.1016/0025-3227(90)90060-W.

McClusky, S., Balassanian, S., Barka, A., Demir, C., Ergintav, S., Georgiev, I., Gurkan, O., Hamburger, M., Hurst, K., Kahle, H., Kastens, K., Kekelidze, G., King, R., Kotzev, V., Lenk, O., Mahmoud, S., Mishin, A., Nadariya, M., Ouzounis, A., Paradissis, D., Peter, Y., Prilepin, M., Reilinger, R., Sanli, I., Seeger, H., Tealeb, A., Toksöz, M. N., and Veis G. 2000. Global Positioning System constraints on plate kinematics and dynamics in the eastern Mediterranean and Caucasus. Journal of Geophysical Research, Solid Earth, **105** : 5695–5719.

McKenzie, D.P. 1972. Active tectonics of the Mediterranean region. Geophysical Journal of the Royal Astronomical Society, **30** : 109-185.

McKenzie, D. P. 1978. Active tectonics of the Alpine Himalayan Belt, the Aegean Sea and surrounding regions. Geophysical Journal of the Royal Astronomical Society, **55** : 217–252.

Mercier, J.-L., Sorel, D., and Simeakis, K. 1987. Change in the state of stress in the overriding plate of a subduction zone: the Aegean Arc from the Pliocene to the present. Annales Tectonicae, **1** : 20-39.

Mercier, J.-L., Sorel, D., Vergely, P., and Simeakis, K. 1989. Extensional tectonic regimes in the Aegean basins during the Cenozoic. Basin Research, **2** : 49-71.

Morris, A., and Anderson, M. 1996. First palaeomagnetic results from the Cycladic Massif, Greece, and their implications for Miocene extension directions and tectonic models in the Aegean. Earth and Planetary Science Letters, **142** : 397-408.

Mposkos, E., and Kostopoulos, D. 2001. Diamond, former coesite and supersilicic garnet in metasedimentary rocks from the Greek Rhodope: a new ultrahigh-pressure metamorphic province established. Earth and Planetary Science Letters, **192** : 497–506.

Müller, M.D., Geiger, A., Kahle, H.-G., Veis, G., Billiris, H., Paradissis, D., and Felekis, S. 2013. Velocity and deformation fields in the North Aegean domain, Greece, and implications for fault kinematics, derived from GPS data 1993–2009. Tectonophysics, **597-598** : 34–49. http://dx.doi.org/10.1016/j.tecto.2012.08.003

Nagel, T. J., Schmid, S., Janak, M., Froitzheim, N., Jahn-Awe, S., and Georgiev, N. 2011. The exposed base of a collapsing wedge: The Nestos Shear Zone (Rhodope Metamorphic Province, Greece). Tectonics, **30** : TC4009, doi: 10.1029/2010TC002815.

Nyst, M., and Thatcher, W. 2004. New constraints on the active tectonic deformation of the Aegean. Journal of Geophysical Research, Solid Earth, **109** : B11406, doi:10.1029/2003JB002830.

Papanikolaou, D.J., and Royden, L.H. 2007. Disruption of the Hellenic arc: Late Miocene extensional detachment faults and steep Pliocene-Quaternary normal faults—Or what happened at Corinth? Tectonics, **26** : TC5003. doi:10.1029/2006TC002007.

Papanikolaou, D., Alexandri. M., and Nomikou. P. 2006. Active faulting in the north Aegean basin. in Dilek Y. and Pavlides S. eds. Postcollisional tectonics and magmatism in the Mediterranean region and Asia: Geological Society of America, Special Paper, **409** : 189-209. doi: I 0.1130n006.2409(ll).

Papanikolaou, D., Alexandri, B., Nomikou, P., and Ballas, D. 2002. Morphotectonic structure of the western part of the North Aegean Basin based on swath bathymetry. Marine Geology, **190** : 465–492.

Parra, T., Vidal, O., and Jolivet, L., 2002. Relation between the intensity of deformation and rétrogression in blueschist metapelites of Tinos Island (Greece) evidenced by chlorite–mica local equilibria. Lithos, **63** : 41– 66.

Piromallo, C., and Morelli, A., 2003. P wave tomography of the mantle under the Alpine-Mediterranean area. Journal of Geophysical Research, **108,** 2065, doi:10.1029/2002JB001757.

Philippon, M., Brun, J.P., and Gueydan F. 2012. Deciphering subduction from exhumation in the segmented Cycladic Blueschist Unit (Central Aegean, Greece). Tectonophysics, **524** : 116-134, doi:10.1016/j.tecto.2011.12.025

Philippon, M., Brun, J.-P., Gueydan, F. and Sokoutis, D. 2014. The interaction between Aegean back-arc extension and Anatolia escape since Middle Miocene. Tectonophysics, **631** : 176–188**,** doi:10.1016/j.tecto.2014.04.039

Piromallo, C., and Morelli, A. 2003. P wave tomography of the mantle under the Alpine-Mediterranean area. Journal of Geophysical Research, Solid Earth, **108** : 2065.

Pourteau, A., Candan, O. and Oberhänsli, R. 2010. High□pressure metasediments in central Turkey: Constraints on the Neotethyan closure history. Tectonics, **29**, TC5004, doi:10.1029/2009TC002650

Ring, U., Okrusch, M., and Will, T. 2007. Samos Island, Part I: metamorphosed and nonmetamorphosed nappes, and sedimentary basins. Journal of the Virtual Explorer, **27** : paper 5. doi:10.3809/jvirtex.2007.00180.

Rosenbaum, G., and Ring, U. 2007. Structure and metamorphism of Amorgos: a field excursion. Journal of the Virtual Explorer, **27** : Paper 7.

Roussos, N. 1994. Stratigraphy and paleogeographic evolution of Palaeocene molassic basins of N. Aegean. Bulletin of the Geological Society of Greece, **XXX** : 275-294.

Roussos, N. and Lyssimachou, T. 1991. Structure of the Central North Aegean Trough: an active strike-slip deformation zone. Basin Research, **3** : 39-48.

Royden, L.H. 1993. The tectonic expression slab pull at continental convergent boundaries. Tectonics, **12** : 629-638.

Royden, L.H. and Papanikolaou, D.J. 2011. Slab segmentation and late Cenozoic disruption of the Hellenic arc. Geochemistry, Geophysics, Geosystems, **12** : Q03010, doi: 10.1029/2010GC003280.

Sakellariou, D., Mascle, J. and Lykousis, V. 2013. Strike slip tectonics and transtensional deformation in the Aegean region and the Hellenic arc: preliminary results. Bulletin of the Geological Society of Greece, XLVII, Proceedings of the 13th International Congress, Chania, Sept. 2013.

Salaün, G. 2011. Structure et déformation du manteau supérieur de la région Egée-Anatolie par tomographie en ondes de Rayleigh. PhD Thesis University of Grenoble.

Salaün, G., Pedersen, H., Paul, A., Farra, V., Karabulut, H., Hatzfeld, D., Childs, D.M., Pequegnat, C., and the SIMBAAD Team 2012. High-resolution surface wave tomography beneath the Aegean-Anatolia region: constraints on upper mantle structure. Geophysical Journal International, **190** : 406–420. http://dx.doi.org/10.1111/j. 1365-246X.2012.05483.x.

Schueller, S., F. Gueydan, and P. Davy, 2005, Brittle-ductile coupling: Role of ductile viscosity on brittle fracturing. Geophysical Research Letters, **32**, (L10308), doi:10.1029/2004GL022272.

Schueller, S., Gueydan, F., and Davy. P. 2010. Mechanics of the transition from localized to distributed fracturing in layered brittle–ductile systems. Tectonophysics, **484** : 48–59. doi:10.1016/j.tecto.2009.09.008

Sengör, A.M.C., Tüysüz, O., Imren, C., Sakınç, M., Eyidogan, H., Görür, N., Le Pichon, X., and Rangin, C. 2005. The North Anatolian Fault: A New Look. Annual Review of Earth and Planetary Sciences, **33** : 37–112.

Shaked, Y., Avigad, D., Garfunkel, Z. 2000. Alpine high-pressure metamorphism at the Almyropotamos window (southern Evia, Greece). Geological Magazine, **137** : 367–380.

Siyako, M., and Huvaz, O. 2007. Eocene stratigraphic evolution of the Thrace Basin, Turkey. Sedimentary Geology, **198** : 75–91.

Snel, E., Marunteanu, M., and Meulenkamp, J.E. 2006. Calcareous nannofossil biostratigraphy and magnetostratigraphy of the Upper Miocene and Lower Pliocene of the Northern Aegean (Orphanic Gulf-Strimon Basin areas), Greece. Palaeogeography, Palaeoclimatology, Palaeoecology, **238** : 125 - 150, doi: 10.1016/j.palaeo.2006.03.022.

Sokoutis, D., Brun, J.-P., Van Den Driessche, J., and Pavlides, S. 1993. A major Oligo-Miocene detachment in southern Rhodope controlling north Aegean extension. Journal of the Geological Society, London, **150** : 243-246.

Sözbilir, H., Sarı, B., Uzel, B., Sümer, Ö., and Akkiraz, S. 2011. Tectonic implications of transtensional supradetachment basin development in an extension-parallel transfer zone:

the Kocaçay Basin, western Anatolia, Turkey. Basin Research, **23** : 423–448. http://dx.doi.org/10.1111/j.1365-2117.2010.00496.x.

Taymaz, T., Jackson, J., McKenzie, D., 1991. Active tectonics of the north and central Aegean Sea. Geophysical Journal International, **106** : 433–490.

Thomson, S.N., Stoeckhert, B., and Brix, M.R. 1998. Thermochronology of the high-pressure metamorphic rocks of Crete, Greece; implications for the speed of tectonic processes. Geology, **26** : 259–262.

Tirel, C., Gueydan, F., Tiberi, C., and Brun, J.-P. 2004. Aegean crustal thickness inferred from gravity inversion. Geodynamical implications. Earth and Planetary Science Letters, **228** : 267-280.

Tirel, C., Brun, J.-P., and Sokoutis, D. 2006. Extension of thickened and hot lithospheres: Inferences from laboratory modeling. Tectonics, **25**: TC1005, doi:10.1029/2005TC001804

Tirel, C., Brun, J.-P., and Burov, E. 2008. Dynamics and structural development of metamorphic core complexes. Journal of Geophysical Research, **113** : B04403, doi:10.1029/2005JB003694

Tirel, C., Brun, J.-P., Burov, E., Wortel, M., and Lebedev, S. 2013. A plate tectonics oddity: Caterpillar-walk exhumation of subducted continental crust. Geology, **41** : 555-558.

Urai, V.L., Shuiling, R.D., and Jansen, J.B.H. 1990. Alpine deformation on Naxos (Greece). In: Knipe, R.J., Rutter, E.H. (Eds.), Deformation Mechanisms, Rheology and Tectonics Geological Society, Special Publications, **54** : 509–522.

Uzel, B, Sözbilir, H., Özkaymak, C, Kaymakcı, N., and Langereis, C.G. 2013. Structural evidence for strike-slip deformation in the İzmir–Balikesir transfer zone and consequences for late Cenozoic evolution of western Anatolia (Turkey). Journal of Geodynamics, **65** : 94-116.

Uzel, B., Langereis, C.G., Kaymakci, N., Sözbilir, H., Özkaymak, Ç., and Özkaptan, M. 2015. Paleomagnetic evidence for an inverse rotation history of Western Anatolia during the exhumation of Menderes core complex. Earth and Planetary Science Letters, **414** : 108-125.

van Hinsbergen, D.J.J., 2010. A key extensional metamorphic complex reviewed and restored: The Menderes Massif of western Turkey. Earth Sciences Review, **102** : 60–76, doi:10.1016/j.earscirev.2010.05.005.

van Hinsbergen, D.J.J., and Schmid, S.M. 2012. Map view restoration of Aegean–West Anatolian accretion and extension since the Eocene. Tectonics, **31** : TC5005, doi:10.1029/2012TC003132.

van Hinsbergen, D.J.J., Langereis, C.G., and Meulenkamp, J.E. 2005. Revision of the timing, magnitude and distribution of Neogene rotations in the western Aegean region. Tectonophysics, **396** : 1–34. doi: 10.1016/j.tecto.2004.10.001.

van Hinsbergen, D.J.J., Dekkers, M. J., Bozkurt, E. and Koopman, M., 2010. Exhumation with a twist: Paleomagnetic constraints on the evolution of the Menderes metamorphic core complex, western Turkey. Tectonics, **29** , TC3009, doi:10.1029/2009TC002596.

Wawrzenitz, N., and Krohe, A. 1998. Exhumation and doming of the Thasos metamorphic core complex (S Rhodope, Greece): structural and geochronological constraints. Tectonophysics, **285** : 301-332.

Weidmann, M., Solounias, N., Drake, R.E., and Curtis, G.H., 1984. Neogene stratigraphy of the eastern basin, Samos Island, Greece. Geobios, **17** : 477 -490.

Widiyantoro, S., van der Hilst, R.D., and Wenzel F. 2004. Deformation of the Aegean Slab in the Mantle Transition Zone. International Journal of Tomography & Statistics, **D04** :1-14. December 2004 ISSN 0972-9976;

Wortel, M.J.R., and Spakman, W. 2000. Subduction and slab detachment in the

Mediterranean–Carpathian region. Science, **290** : 1910–1917.
Wuthrich, E. 2009. Low temperature thermochronology of the North Aegean Rhodope Massif, Ph.D. thesis, Swiss Federal Institute of Technology, Zurich.

Figure captions

Fig. 1. Simplified geological map of the Aegean domain in Tertiary showing the three main continental blocks, Rhodopia, Pelagonia and Adria, separated by the Vardar and Pindos suture zones. The cross-section shows the present-day crustal-scale structure of the Aegean domain and the geometry of the Hellenic subduction. NAF: North Anatolian Fault. NAT: North Aegean Through. MIF: Myrthes-Ikaria Fault.

Fig. 2. Distribution of Paleogene (a) and Neogene (b) basins in the Aegean domain. Acronyms same as in Figure 1.

Fig. 3. The two core complexes (High-temperature metamorphism) of the Aegean domain. SRCC: Southern Rhodope Core Complex, which exhumed between 45 Ma and 18 Ma and whose detachment dip southwestward. CCCC: Central Cyclades Core Complex, whose exhumation history is shown by a PTt diagram from Naxos (Numbers in circles: Time in My) (After Duchêne et al. 2006 in Jolivet and Brun 2010) and whose detachment dip northeastward to the West and Northward to the East. Red arrows: syn-metamorphic senses of shear. Senses of shear associated to core complex extension after Sokoutis et al (1993) and Brun and Sokoutis (2007) for the SRCC and Gautier et al (1993) and Gautier and Brun (1994) for the CCCC.

Fig. 4. High-pressure metamorphism in the Adria and Pelagonia blocks. PTt diagrams illustrate the exhumation history of the Cycladic Blueschist Unit in Tinos (Numbers in circles: Time in My) (After Parra et al. 2002 in Jolivet and Brun 2010) and of the " Phyllite–Quartzite Nappe » in Peloponnese (Numbers in circles: Time in My) (After Jolivet et al. 2010*a*). Black

arrows: sense of shear related to subduction. White arrows: sense of shear related to exhumation. Senses of shear associated to subduction (black arrows) after Huet et al (2009) and Philippon et al (2012). Senses of shear associated to exhumation (white arrows) after Gautier and Brun (1994) for the Cyclades and Jolivet et al (2010a) for the Peloponnese and Crete.

Fig. 5. Frequency distribution histograms of low-temperature thermochronology ages (apatite and zircon fission tracks (AFT and ZFT) and UTh/He on apatite and zircon) in Rhodope (data from Wuthrich 2009), Cyclades (Compilation of data: Philippon et al. 2012) and Peloponnese-Western Crete (data from Brix et al. 2002; Marsellos et al. 2014). Numbers correspond to the number of ages within a bin.

Fig. 6. Major strike-slip faults and sedimentary basins in the Aegean Sea, as displayed by bathymetry (GMRT bathymetry data from Carbotte et al. 2004). The Myrthes-Ikaria fault that connects the Myrthes and Ikaria basins (Philippon et al. 2012, 2014) is the offshore extend of the onshore Izmir-Balikeshir Transfer Zone (Sozbilir et al. 2010), located between the Izmir-Ankara suture zone and the Menderes Massif (pink).

Fig. 7. Present-day displacements (after Nyst and Thatcher 2004) superposed to the map of Neogene basins (Yellow) showing that a major change occurred in the course of post-Middle Miocene deformation when the North Anatolian Fault (NAF) localized and connected to the North Aegean Through (NAT).

Fig. 8. Change in the principal direction of stretching between Pliocene to Lower (?) Pleistocene (a) and Lower (?) Pleistocene to Present (b) related to the localization of the

North Anatolian Fault in the North Aegean (Principal directions of stretching after Lyberis 1984; Bathymetry data GMRT from Carbotte et al. 2004).

Fig. 9. Restoration of Aegean extension in map view at 5, 15, 30 and 45 Ma. Colours of continental blocks and suture zones same as in Figure 1. Orange: Paleogene basins (MHT: Mid Hellenic Trough; XB: Xanthi Basin; TB: Thrace Basin). Yellow: Neogene basins; only shown in the present-day map (e). Red and white arrows (in b to e): principal direction of stretching and sense of shear related to exhumation of high-temperature (core complexes) and high-pressure metamorphic rocks, respectively (See Figs. 3 and 4). Black arrows (in a): principal direction of stretching and sense of shear related to subduction of Adria, in their position at the onset of extension at 45 Ma. Top-to-SW shear in the SRCC (Red arrows in b to e) and top-to-NE shear in blueschists (White arrows in b to e) started to develop at 45 Ma. Top-to-NE shear in the CCCC (Red arrows in c to e) started to develop prior to 20.7 Ma. All arrows, except the black ones, are represented at all stages following their initial development as their final position reflect block rotations.

Fig. 10. Restoration of Aegean extension along two NE-SW trending lithosphere-scale cross-sections AA' and BB' (see location on map). Shape of the Hellenic slab (in sections) and geometry of the slab tear (map view) from the S-wave tomographic model of Salaün (2011). The slab tear of section AA' passes to a fold in section BB' (See slab tear contours in red on map). At 45 Ma, the restoration shows the geometry of the thrust wedge resulting from the pilling up of Rhodopia (Brown), Pelagonia (Purple) and Adria (Blue) continental blocks separated by the suture zones of the Vardar (Green) and the Pindos (Orange). Extension that is a direct function of the amount of trench retreat is much larger in section AA' than in section BB' where it is mostly located to the North of the Vardar suture zone.

Fig. 11. Rate of trench retreat along section AA' (Fig.10) showing an acceleration by a factor 5 since Middle Miocene, from 0.6 to 3.2 cm y^{-1}, that correlates i) with a change in the mode of extension from localized/stage 1 (exhumation of HT and HP metamorphic rocks) to distributed/stage 2 (segmentation of exhumed metamorphic units and deposition of Neogene basins over the whole Aegean domain) and ii) with the strong contrast in shape and distribution of Paleogene and Neogene basins (Fig. 2).

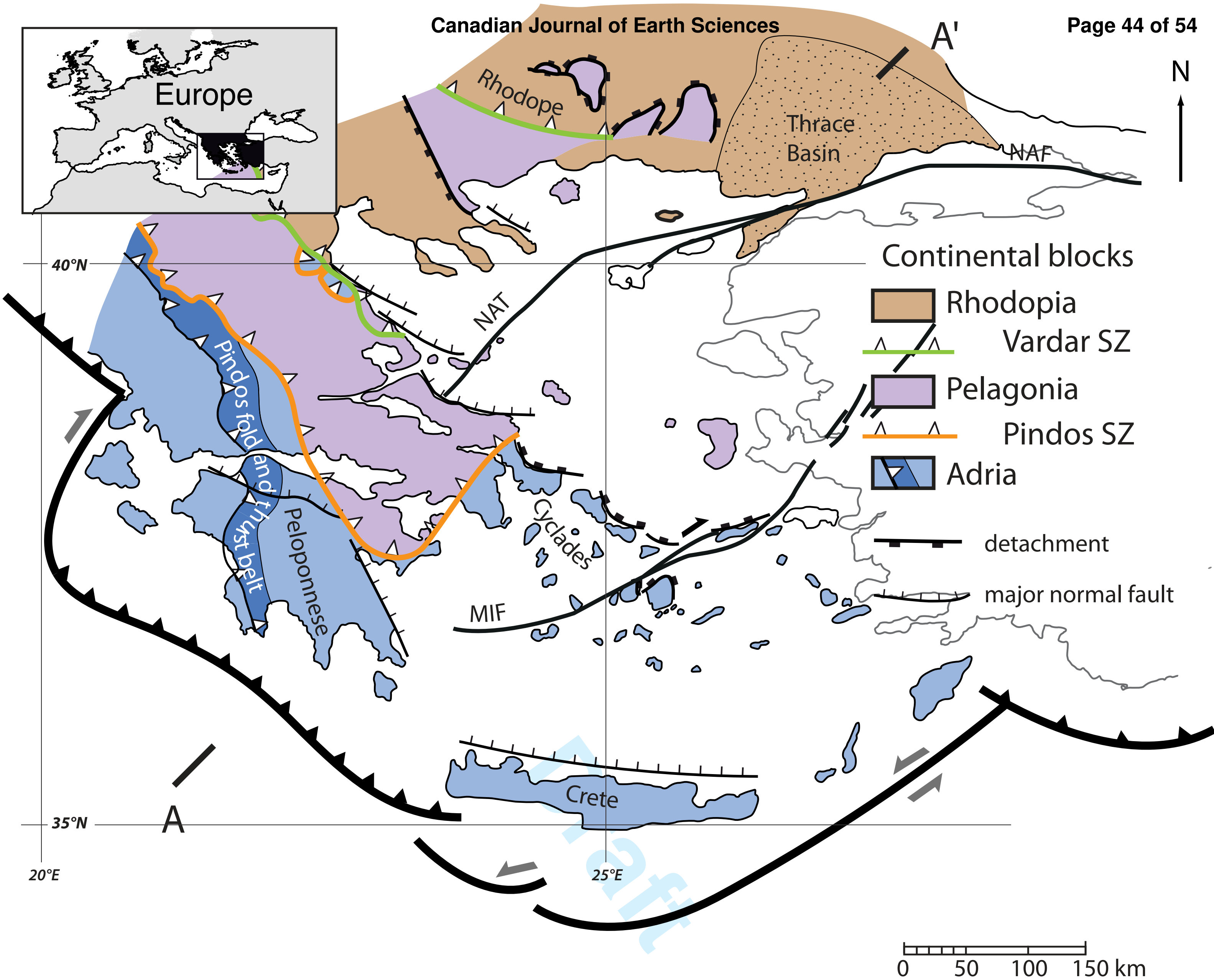

Europe
Rhodope
Thrace Basin
NAF
NAT
MIF
Cyclades
Pindos fold and thrust belt
Peloponnese
Crete
A
A'
N
40°N
35°N
20°E
25°E
Continental blocks
Rhodopia
Vardar SZ
Pelagonia
Pindos SZ
Adria
detachment
major normal fault
0
50
100
150 km

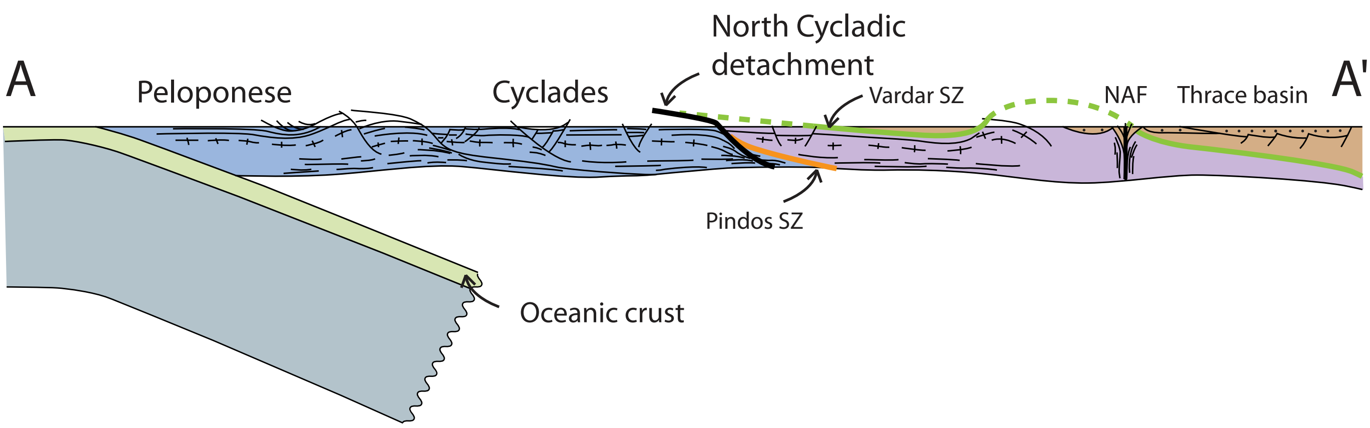

A
A'
Peloponese
Cyclades
North Cycladic detachment
Vardar SZ
NAF
Thrace basin
Pindos SZ
Oceanic crust

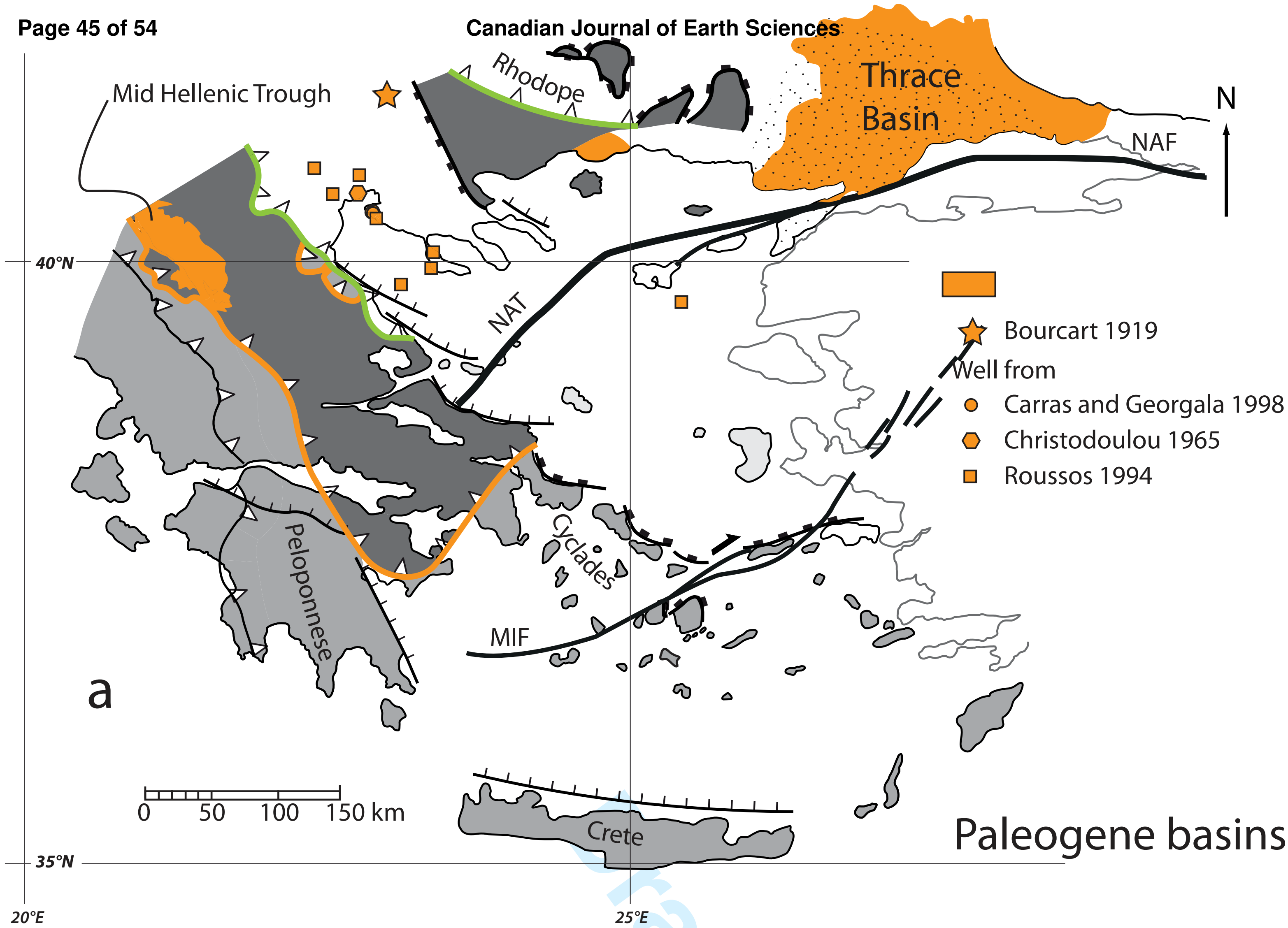

Mid Hellenic Trough
Rhodope
Thrace Basin
N
NAF
40°N
NAT
Bourcart 1919
Well from
Carras and Georgala 1998
Christodoulou 1965
Roussos 1994
Cyclades
Peloponnese
MIF
a
0 50 100 150 km
Crete
Paleogene basins
35°N
20°E
25°E

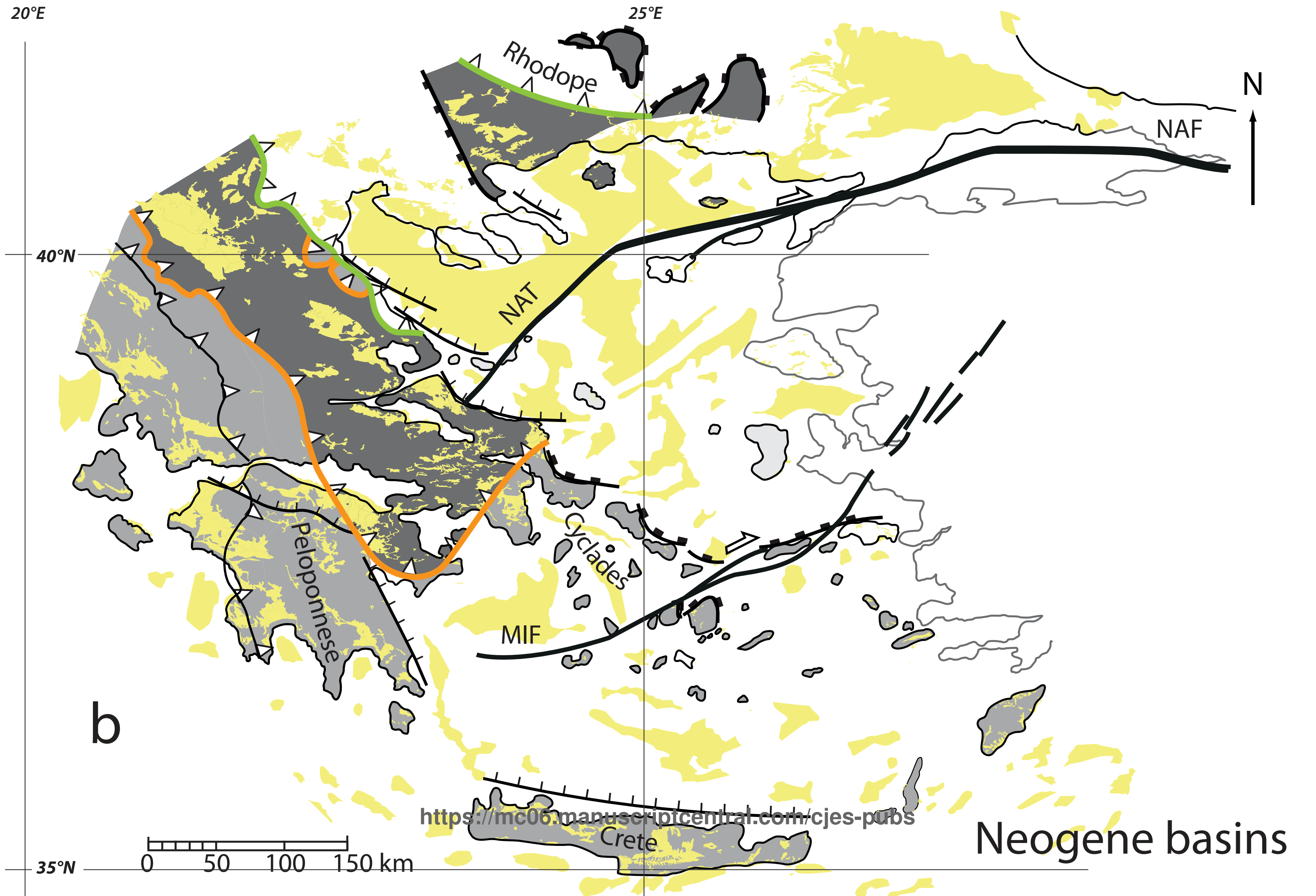

20°E
25°E
Rhodope
N
NAF
40°N
NAT
Cyclades
Peloponnese
MIF
b
Crete
0 50 100 150 km
Neogene basins
35°N

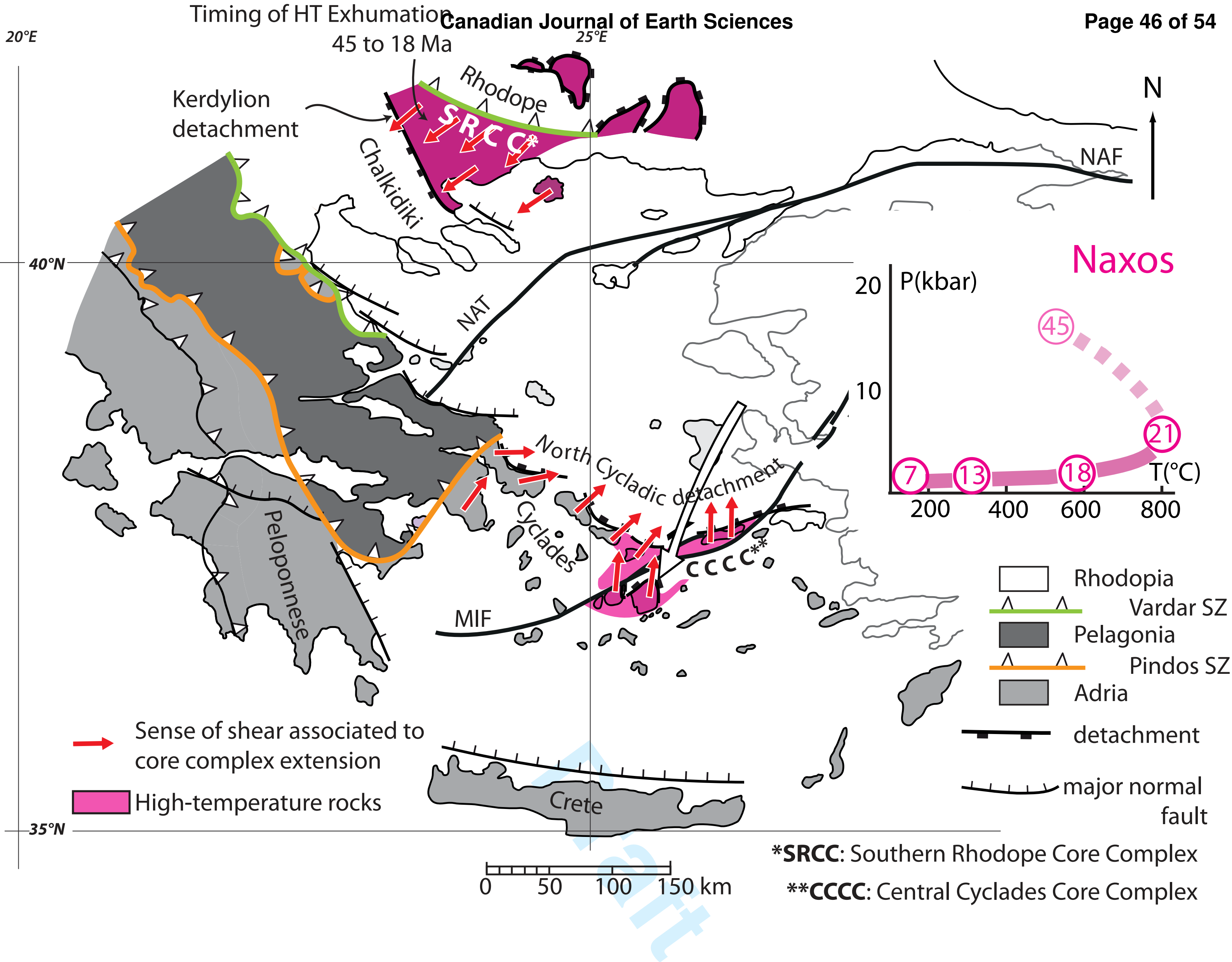
Timing of HT Exhumation
45 to 18 Ma
20°E
25°E
Kerdylion
detachment
Rhodope
SRCC*
Chalkidiki
N
NAF
NAT
40°N
Naxos
20
P(kbar)
10
45
21
7
13
18
T(°C)
200
400
600
800
North Cycladic detachment
Cyclades
CCCC**
Peloponnese
MIF
Rhodopia
Vardar SZ
Pelagonia
Pindos SZ
Adria
detachment
major normal
fault
Sense of shear associated to
core complex extension
High-temperature rocks
Crete
35°N
0
50
100
150 km
*SRCC: Southern Rhodope Core Complex
**CCCC: Central Cyclades Core Complex
Draft

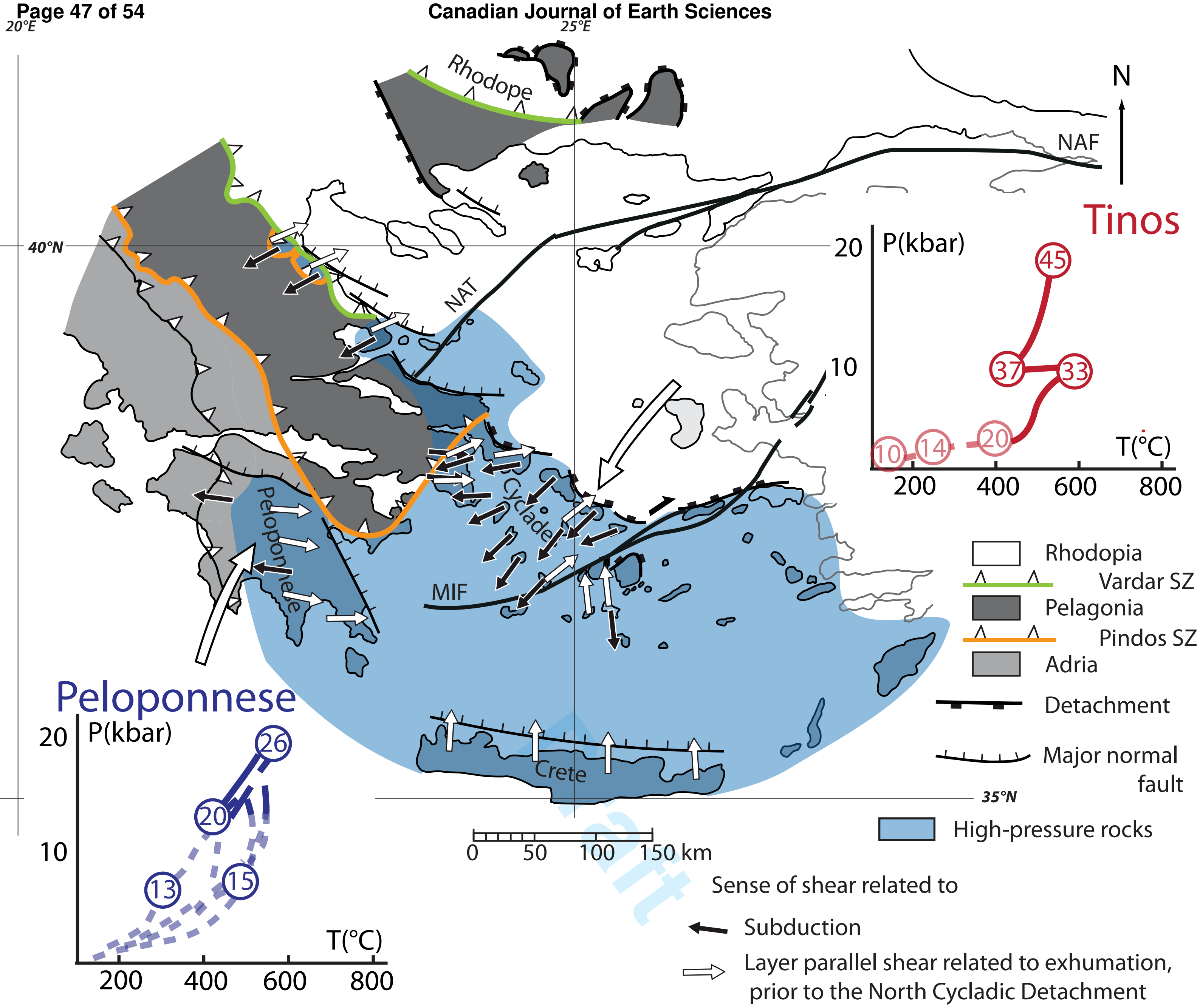
20°E
25°E
40°N
35°N
Rhodope
NAT
NAF
N
MIF
Peloponnese
Cyclades
Crete
Tinos
P(kbar)
20
10
T(°C)
200
400
600
800
45
37
33
10
14
20
Peloponnese
P(kbar)
20
10
T(°C)
200
400
600
800
26
20
13
15
0
50
100
150 km
Rhodopia
Vardar SZ
Pelagonia
Pindos SZ
Adria
Detachment
Major normal fault
High-pressure rocks
Sense of shear related to
Subduction
Layer parallel shear related to exhumation, prior to the North Cycladic Detachment

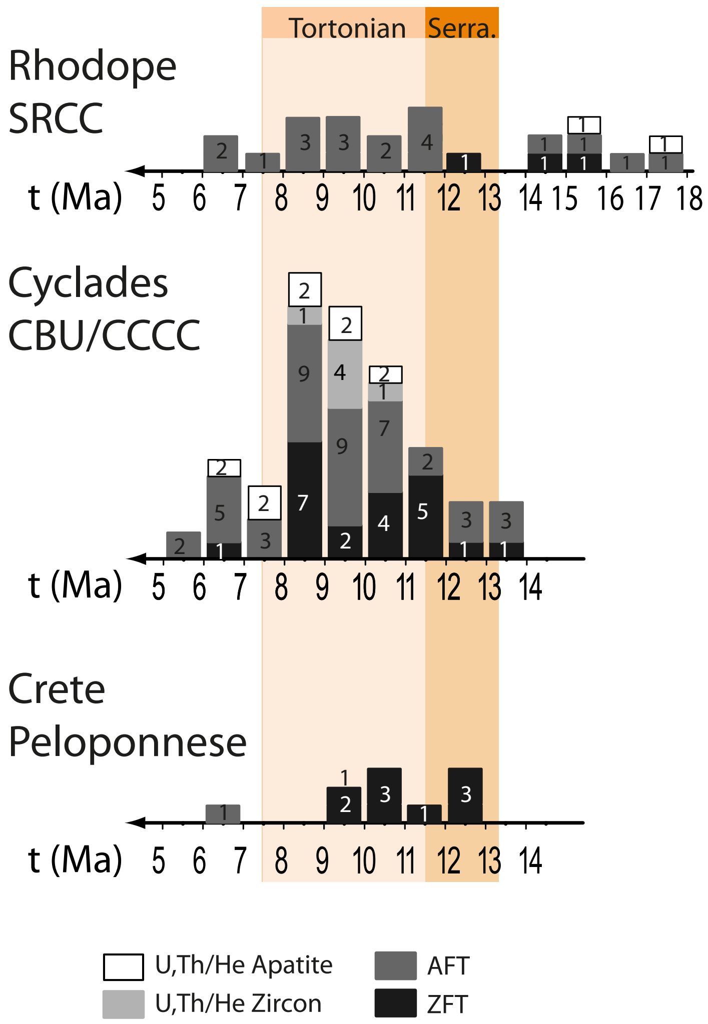
Tortonian
Serra.
Rhodope
SRCC
t (Ma)
Cyclades
CBU/CCCC
t (Ma)
Crete
Peloponnese
t (Ma)
U,Th/He Apatite
U,Th/He Zircon
AFT
ZFT

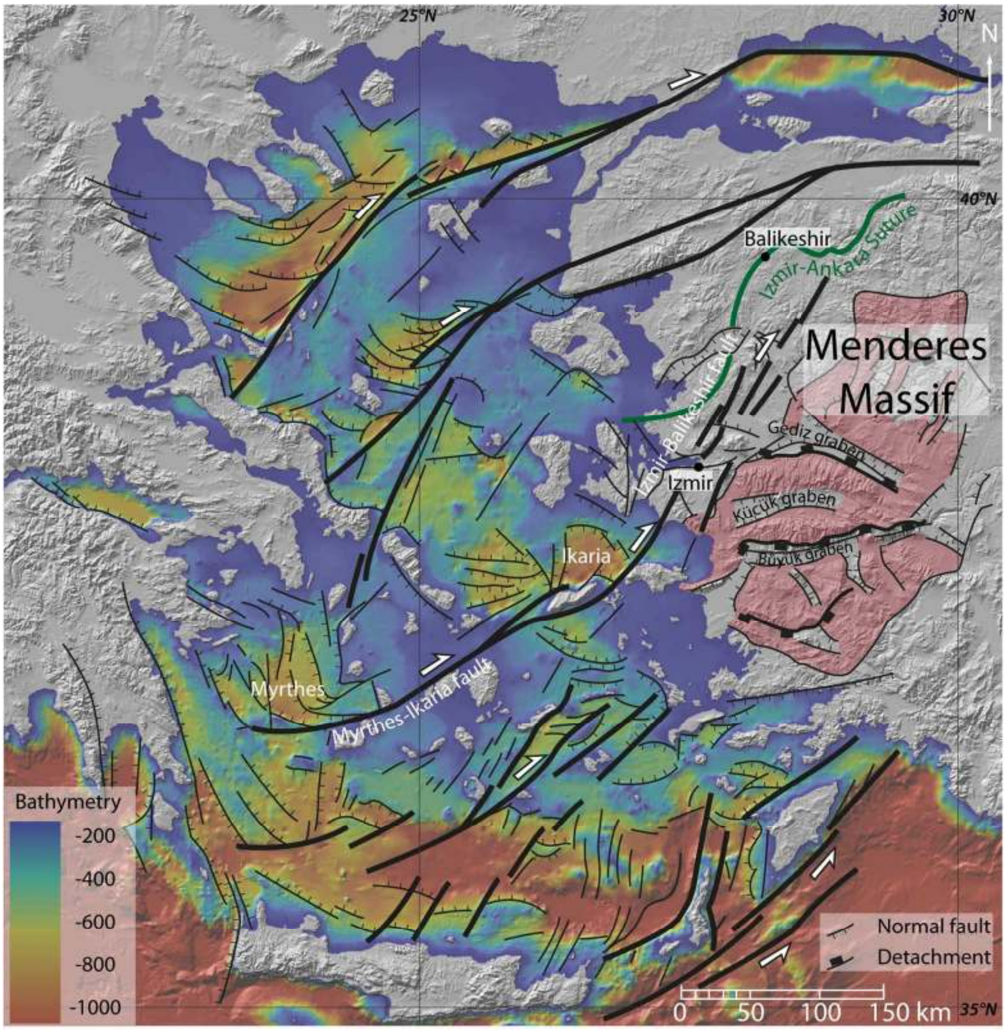

Major strike-slip faults and sedimentary basins in the Aegean Sea, as displayed by bathymetry (GMRT bathymetry data from Carbotte et al. 2004). The Myrthes-Ikaria fault that connects the Myrthes and Ikaria basins (Philippon et al. 2012, 2014) is the offshore extend of the onshore Izmir-Balikeshir Transfer Zone (Sozbilir et al. 2010), located between the Izmir-Ankara suture zone and the Menderes Massif (pink).
418x429mm (100 x 100 DPI)

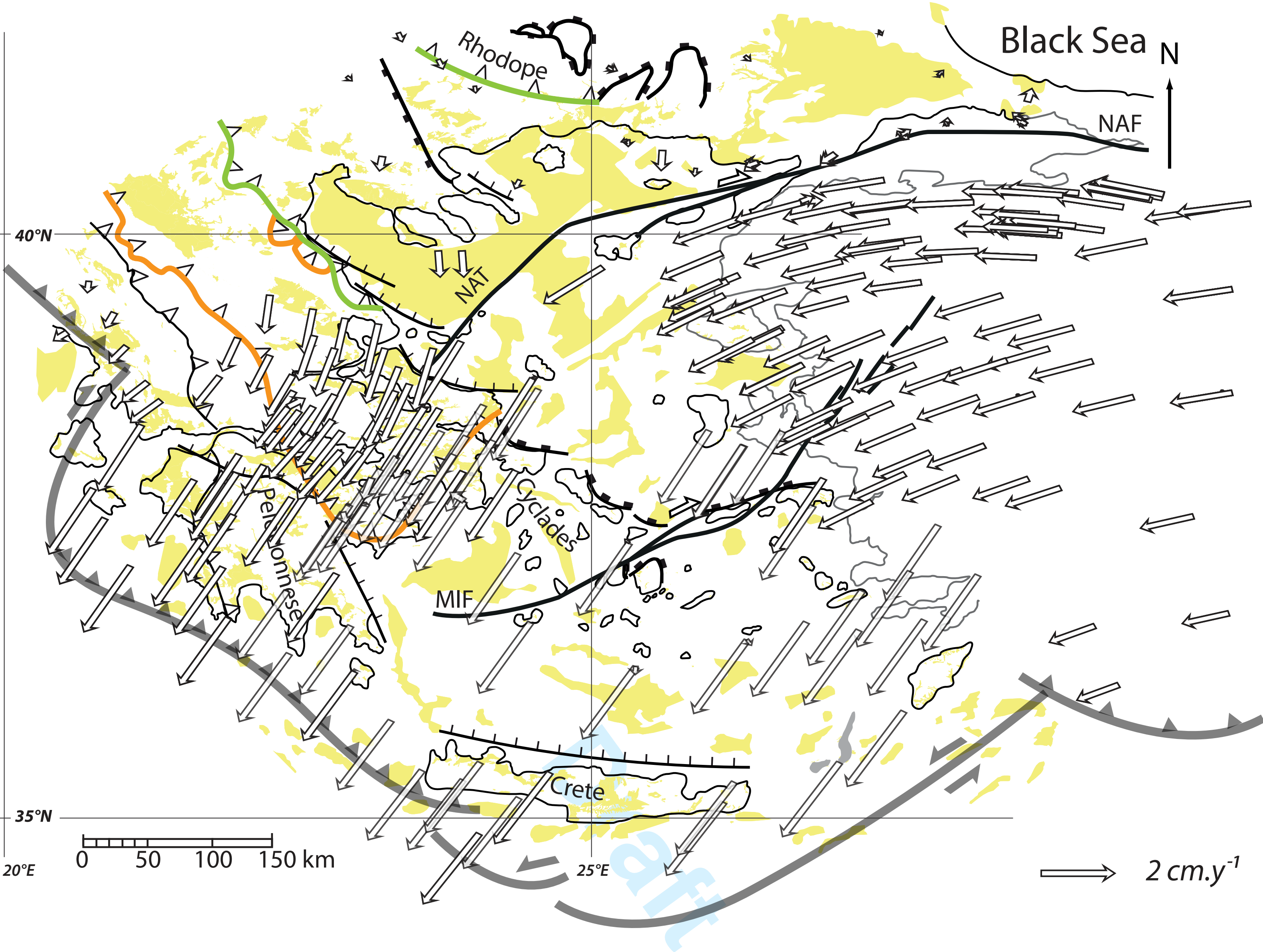
Black Sea
N
NAF
Rhodope
NAT
40°N
35°N
20°E
25°E
Cyclades
Peloponnese
MIF
Crete
0 50 100 150 km
2 cm.y-1

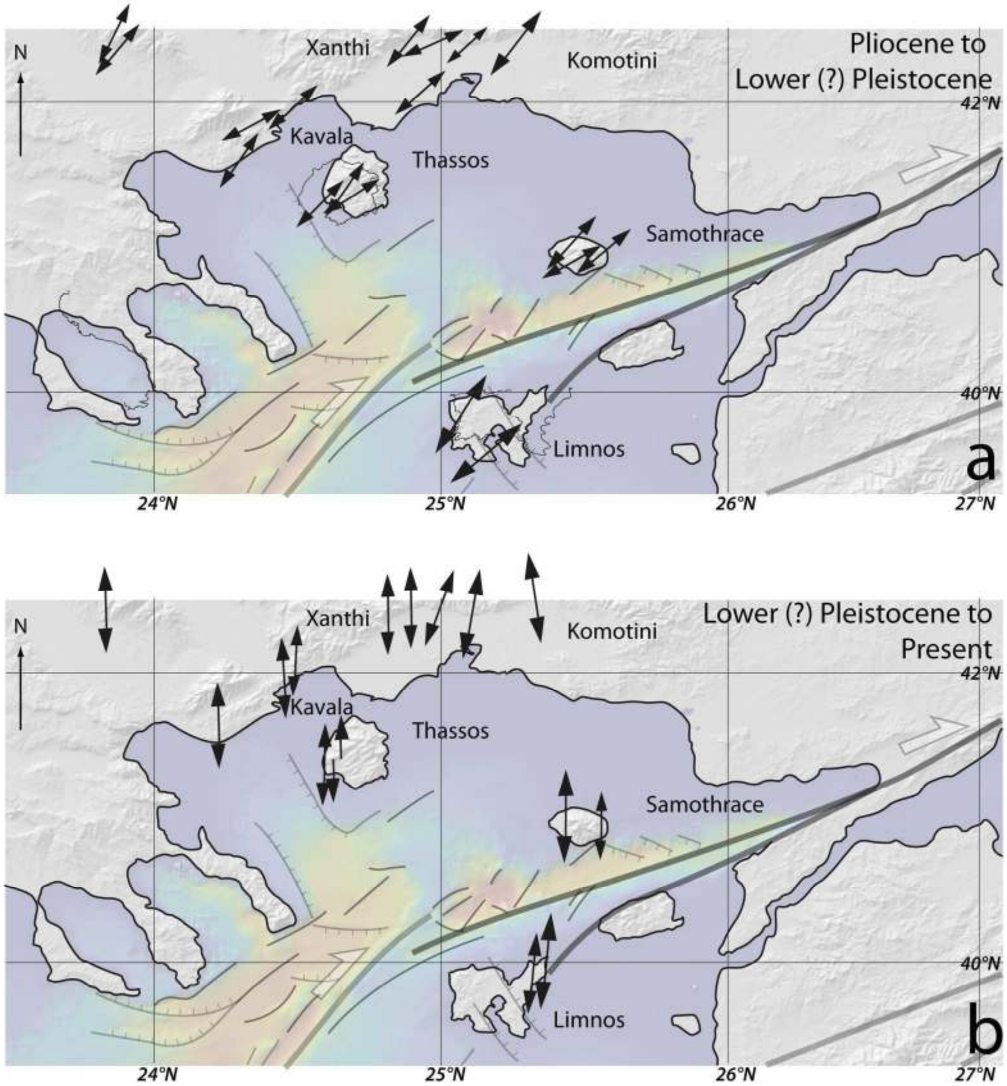

Change in the principal direction of stretching between Pliocene to Lower (?) Pleistocene (a) and Lower (?) Pleistocene to Present (b) related to the localization of the North Anatolian Fault in the North Aegean (Principal directions of stretching after Lyberis 1984; Bathymetry data GMRT from Carbotte et al. 2004).
716x774mm (72 x 72 DPI)

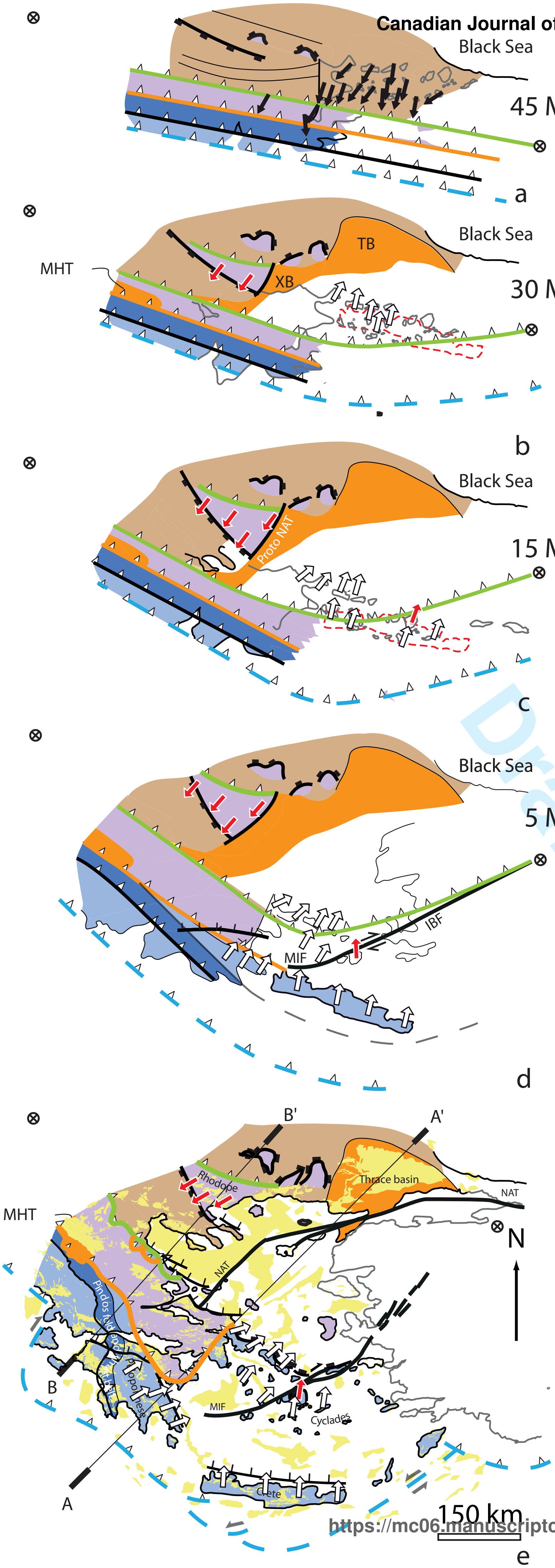
Black Sea
45 Ma
a
MHT
TB
XB
Black Sea
30 Ma
b
Proto NAT
Black Sea
15 Ma
c
Black Sea
5 Ma
IBF
MIF
d
B'
A'
Rhodope
Thrace basin
NAT
N
MHT
NAT
B
MIF
Cyclades
Crete
A
150 km
e

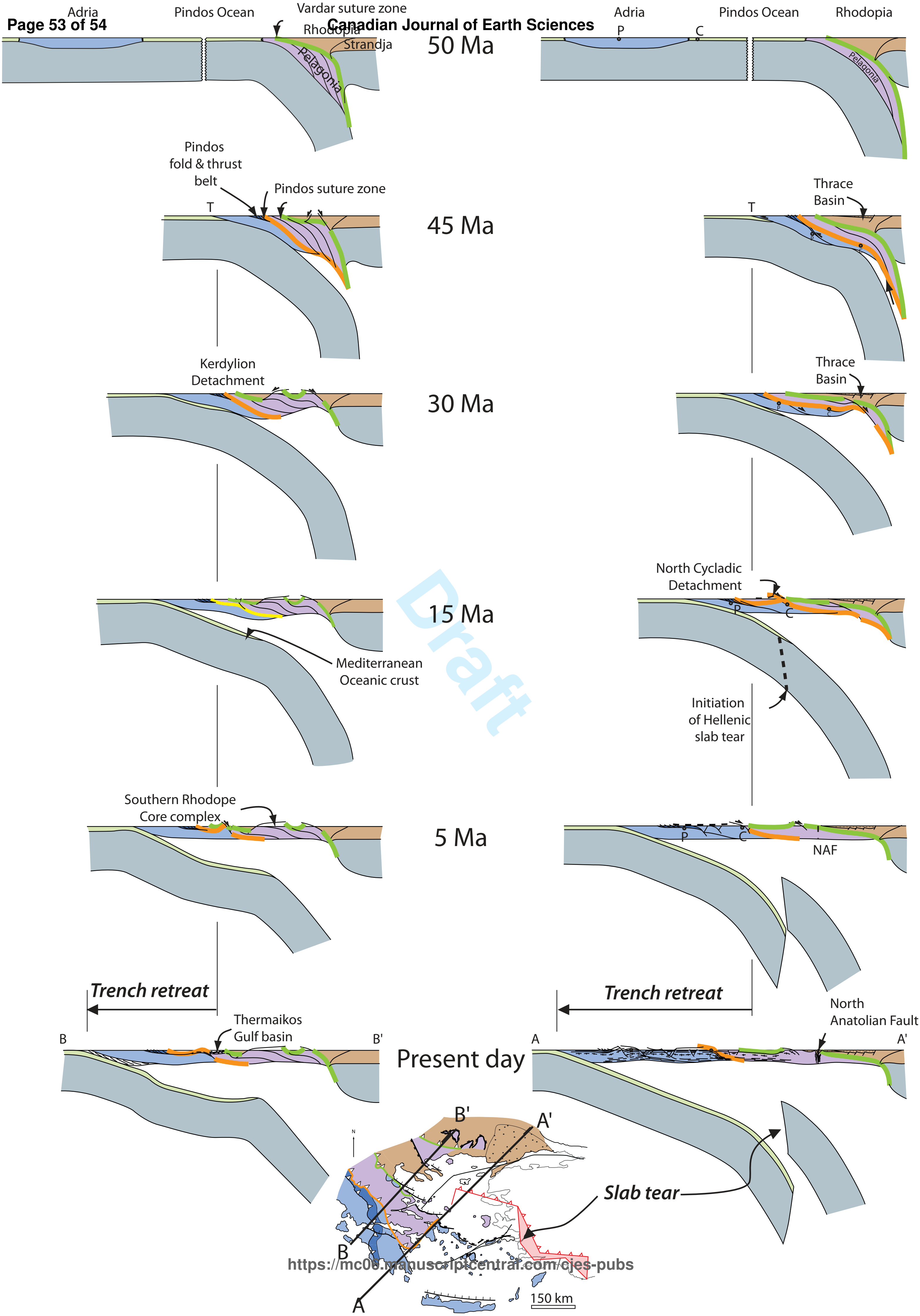

Adria
Pindos Ocean
Vardar suture zone
Rhodopia
Strandja
Pelagonia
50 Ma
Adria
P
C
Pindos Ocean
Rhodopia
Pelagonia
Pindos fold & thrust belt
Pindos suture zone
T
45 Ma
Thrace Basin
T
Kerdylion Detachment
30 Ma
Thrace Basin
North Cycladic Detachment
15 Ma
Mediterranean Oceanic crust
P
C
Initiation of Hellenic slab tear
Southern Rhodope Core complex
5 Ma
P
C
NAF
Trench retreat
Trench retreat
North Anatolian Fault
Thermaikos Gulf basin
B
B'
Present day
A
A'
B'
A'
N
Slab tear
B
A
150 km

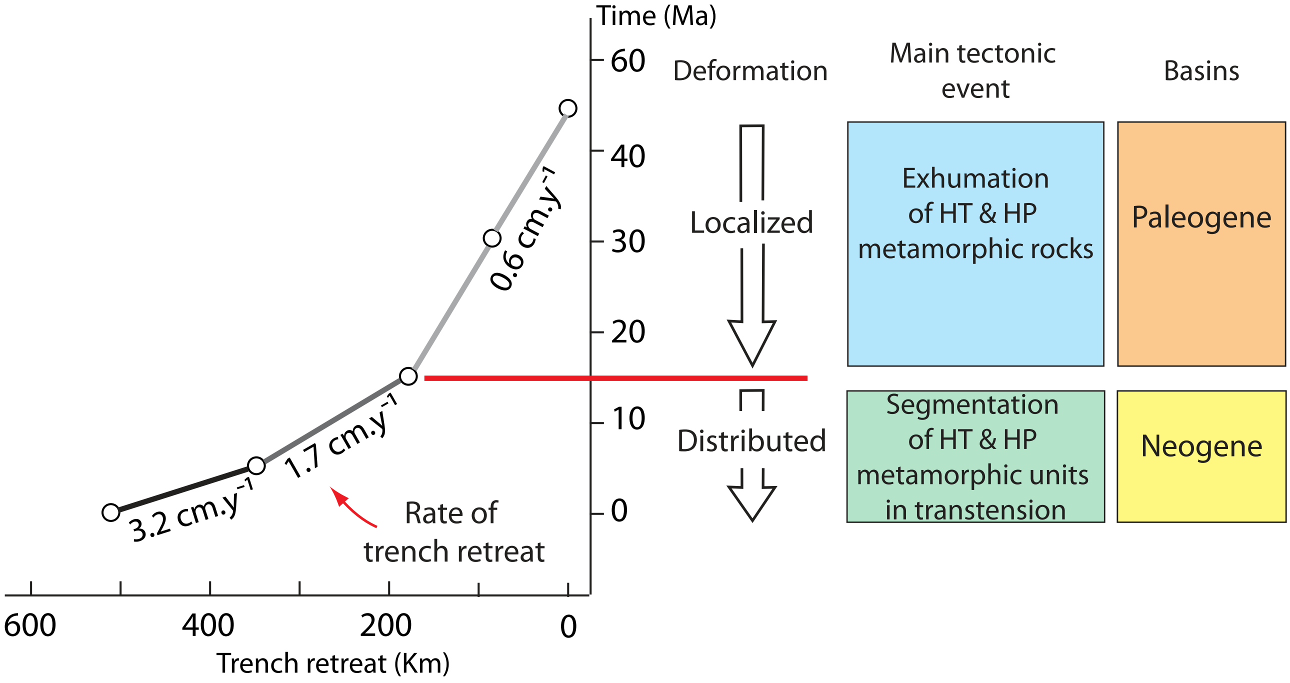

Time (Ma)
60
40
30
20
10
0
0.6 cm.y⁻¹
1.7 cm.y⁻¹
3.2 cm.y⁻¹
Rate of
trench retreat
600
400
200
0
Trench retreat (Km)
Deformation
Localized
Distributed
Main tectonic
event
Exhumation
of HT & HP
metamorphic rocks
Segmentation
of HT & HP
metamorphic units
in transtension
Basins
Paleogene
Neogene